

Copyright is owned by the Author of the thesis. Permission is given for a copy to be downloaded by an individual for the purpose of research and private study only. The thesis may not be reproduced elsewhere without the permission of the Author.

**An Investigation into Nanocellulose Based
Hydrogels for Analgesic Treatment of Avian
Species.**

Thesis presented in partial fulfilment of the
requirement for the degree of

Master of Science

Chemistry

Massey University

Palmerston North, New Zealand

David Bruce Allan

2018

Acknowledgements

Primarily I wish to thank my supervisors, Professor Dave Harding, Dr Preet Singh and Dr Catherine Whitby for their support and tolerance over the course of my studies. Without their patience and understanding this thesis would never have seen the light of day.

Professor Dave Harding. Thank you for always helping me to puzzle through the various problems the project put in our way. Also for tolerating me popping my head in the door multiple times a day with new questions or requests.

Dr Preet Singh, for tolerating the many mishaps and delays in providing HPLC data that would contain mysterious variations and absentee values. Also, the assistance when conducting the chicken trials while you were balancing your time between work and the baby boss.

I also wish to thank Antony Jacob and Rafea Naffa for the double-edged sword of training me to use the HPLC machines, the aid for troubleshooting helped to justify the many sleepless night trying to coax the machine into behaving.

Aline Alberti Morgado. For your help in the chicken sampling, saving me from my needle phobia and providing some laughter after we had only 3 hrs sleep a day I am eternally grateful. Without you the slide into sleep deprived insanity would have been far less enjoyable.

Rixta Stievers. For tolerating the noise in the house as I crawled home at 3 am after long nights of sampling with only the barest rumble of complaint. Also, for never changing the locks when I was out, I know you were tempted.

Joanne Allan. Thank you for the numerous proof readings of my reports, translating the garbled scrawling I produced into legible English helped more than I can say.

For my family, Blod, Kay, Kit and Mungo;

I can never express the degree of my gratitude for showing me support and providing encouragement during my studies. Without you all I would never have made it this far. You gave me a future.

Table of Contents

Abbreviations	vii
List of Figures	viii
List of Tables	ix
List of Graphs.....	ix
1. Abstract	1
2. Literature review	2
2.1 Nanocellulose	2
2.1.1 Nanocellulose forms	2
2.1.2 Cellulose nanocrystals.....	3
2.1.3 Nanofibrillated cellulose	4
2.1.4 TEMPO oxidation	5
2.1.5 Bionanocellulose	6
2.2 Nanocellulose based hydrogels for avian analgesic drug delivery	7
2.3 Enteral routes	8
2.3.1 Oral administration	8
2.3.2 Rectal administration	8
2.3.3 Sub-lingual and buccal administration.....	8
2.4 Parenteral routes	8
2.4.1 Subcutaneous injection	9
2.4.2 Intravenous injection.....	9
2.4.3 Intramuscular injections	9
2.4.4 Topical application.....	10
2.4.5 Intranasal application	10
2.4.6 Blood-brain barrier.....	10
2.5 Traditional hydrogel materials	11
2.5.1 Alginate	11
2.5.2 Chitosan	12
2.6 Hydrogel drug delivery	14
2.6.1 Hydrogels	14
2.6.1.1 Chemical crosslinking.....	15
2.6.1.2 Physical crosslinking.....	16
2.6.1.3 Hydrogel classification	18
2.6.1.4 Smart hydrogels	18
2.6.2 Opioids	19
2.6.2.1 Butorphanol.....	20
2.6.2.2 Avian drug delivery	22

2.6.3 Animal trials.....	23
2.6.3.1 Three R's.....	23
2.7 Biocompatibility issues	24
2.7.1 Non-specific defences	24
2.7.2 Inflammatory response.....	24
2.8 Industrial applications of nanocellulose and bionanocellulose.....	25
2.8.1 Nanoskin	25
2.8.2 Bone repair	26
2.8.3 Nanocellulose drug delivery systems.....	26
2.9 Non-medical industrial applications of hydrogels	27
2.9.1 Soft contact lenses.....	26
2.9.2 Disposable nappies.....	27
2.10 Cellulose harvesting	27
2.11 Analytical techniques	28
2.11.1 Liquid chromatography.....	28
2.11.2 Normal and reverse phase chromatography.....	28
2.11.3 High performance liquid chromatography (HPLC).....	28
2.12 Project Aims.....	29
3. Methodology	30
3.1 Nanocellulose preparation.....	33
3.1.1 Chemical preparation top down approach	33
3.1.2 Biological preparation.....	33
3.1.3 TEMPO	35
3.2 Hydrogel preparation	35
3.2.1 Sodium alginate mixed hydrogels.....	35
3.2.2 Chitosan mixed hydrogels.....	35
3.2.3 Dry NC-SA hydrogel swelling and release patterns	35
3.2.4 NC-SA hydrogel gel preparation	37
3.2.4.1 Preparation of hydrogel for animal testing	37
3.2.4.2 Preparation NC-SA hydrogels for drug release in RO H ₂ O.....	37
3.2.4.3 Preparation of chitosan-SA hydrogels for drug release in RO H ₂ O ...	38
3.2.5 Hydrogel drug release in RO H ₂ O	38
3.3 Avian testing	38
3.3.1 Animal trials.....	38
3.3.2 Drug administration	39
3.3.3 Serum collection	39
3.4 Sample preparation	40

3.4.1 HPLC analysis preparation	40
3.4.2 Solid phase extraction	40
3.4.3 HPLC preparation protocol	41
3.4.4 HPLC run protocol	41
3.4.5 HPLC cleaning protocol	41
3.5 HPLC Validity	42
3.5.1 Butorphanol recovery	42
3.5.2 HPLC specificity	42
3.5.3 HPLC analysis	42
3.5.4 Chromatograph analysis	42
3.5.5 New Column	43
3.5.6 HPLC Linearity	43
3.6 Data analysis	43
3.6.1 Statistical analysis	44
3.6.2 Pharmacokinetic analysis	44
4. Results and discussion	45
4.1 Pre-TEMPO chemical preparation	45
4.2 Bionanocellulose preparation	46
4.3 TEMPO oxidation	48
4.4 Nanocellulose optimisation	50
4.5 Hydrogel preparation	50
4.5.1 Dry NC-SA hydrogel swelling patterns	51
4.5.2 Wet NC-SA hydrogel preparation	53
4.5.2.1 Pilot study	53
4.5.2.2 Primary study preparation	54
4.5.3 Hydrogel release in RO H ₂ O	54
4.5.4.1 NC-SA gel release	56
4.5.4.2 Chitosan-nanocellulose hydrogel release	59
4.6 Animal trials	59
4.6.1 Sample collection issues	62
4.7 Serum analysis	63
4.8 HPLC	63
4.8.1 SPE	63
4.8.2 HPLC Run Protocol	64
4.8.3 HPLC Analysis	65
4.8.4 New column	67
4.8.5 HPLC cleaning protocol	67

4.8.6 HPLC sampling problems	67
4.9 HPLC validation	68
4.9.1 HPLC linearity	68
4.9.2 HPLC specificity.....	69
4.10 Primary Study	73
4.10.1 Gel release rate.....	73
4.10.2 Pharmacokinetic analysis	74
5. Conclusion	80
6. Future Work.....	81
7. References.....	85
8. Appendices.....	90
Appendix i. Timesheets for chicken sampling (Gel).	90
Appendix ii. Timesheets for chicken sampling (No Gel).	92

Abbreviations

AUC – Area under curve

AUMC – Area under the first moment

BBB – Blood-brain barrier

BNC – Bacterial nanocellulose

Ca²⁺ - Calcium ion

Cl/F – Clearance of drug

C_{max} – Maximum plasma concentration

CNC – Cellulose nanocrystals

CNF – Cellulose nanofibrils

COO⁻ - Carboxylate group

DAMPs – Damage associated membrane patterns

G. xylinus – Glucanoacetobacter xylinus

GIT – Gastrointestinal tract

HPLC – High performance liquid chromatography

IPN – Inter-penetrating network

lambda_z – Elimination rate constant

LD₅₀ – The lethal dose for 50% of the test group

MRT – Mean residence time

NC –Nanocellulose

NSAIDs – Non-steroidal anti-inflammatory drugs

PAMPs – Pathogen associated membrane patterns

PRR – Pattern recognition receptor

SA – Sodium alginate

SPE – Solid phase extraction

t_{1/2} – Half-life

TEMPO – 2,2,6,6-Tetramethylpiperidine-1-oxyl

T_{max} – Time when C_{max} occurred

UDP – Uridine diphosphate

UV – Ultraviolet light

List of Figures

1. Untreated hemp fibres	2
2. Images of CNC, CNF and BNC	3
3. TEMPO oxidation cycle.....	5
4. Tempo oxidised cellulose.....	5
5. Biosynthetic pathway for cellulose production	6
6. Subcutaneous injection technique	9
7. Intramuscular injection technique.....	9
8. Blood brain barrier delivery strategies.....	10
9. Alginic acid.....	11
10. Sodium alginate.....	11
11. Deacetylated chitosan structure	12
12. Deacetylation of chitin.....	13
13. Calcium chloride crosslinked sodium alginate	16
14. Hydrogen bonding between sodium alginate.....	17
15. Butorphanol tartrate chemical structure.....	20
16. Wound treated with nanoskin	25
17. Hemp fibres post NaClO ₂ treatment	34
18. <i>G. xylinus</i> culture in GYC media.....	34
19. Biocellulose pellicle	35
20. Purified nanocellulose.....	36
21. TEMPO oxidation of cellulose	48
22. TEMPO oxidise cellulose crosslinked with sodium alginate	49
23. Chicken neck 30 after injection with butorphanol hydrogel.....	61
24. Chicken neck 30 min after injection with commercial butorphanol.....	61

List of Tables

1. Summary of opioid receptor ratios in multiple species.....	21
2. Chicken dosage	40
3. TEMPO oxidation run yields	49
4. Butorphanol standard solutions with variance and percentage variance	56
5. HPLC results from hydrogel release rates within RO H ₂ O with various CaCl ₂ concentrations of crosslinking	58
6. Intra-day variation.....	69
7. Summary of pharmaceutical analysis, hydrogel injection, <i>primary</i> study.....	76
8. Summary of pharmaceutical analysis, commercial butorphanol injection, <i>primary</i> study.....	76

List of Graphs

1. Butorphanol standard curve area	55
2. Butorphanol standard curve height	55
3. Butorphanol concentration calculated from the peak height vs time for hydrogels with various CaCl ₂ concentrations	57
4. Butorphanol concentration calculated from the peak area vs time for hydrogels with various CaCl ₂ concentrations	57
5. Butorphanol stand curve 15.6 ng/mL to 1 mg/mL area	69
6. Butorphanol stand curve for 125 ng/mL 250 ng/mL and 500 ng/mL vs HPLC peak area	70
7. Butorphanol stand curve for 125 ng/mL 250 ng/mL and 500 ng/mL vs HPLC peak height.....	70
8. Chromatograph of four butorphanol spiked plasma standards including blank plasma	71
9. Chromatograph of the three butorphanol standards in mobile phase.....	72
10. Chromatograph of serum from the chickens injected with commercial butorphanol solution	77
11. Chromatograph of serum, chickens injected with the NC:SA hydrogel... ..	78
12. Semi-Log graph comparing the butorphanol concentrations of the various serum samples.....	79

1. Abstract

Drug delivery techniques are an integral component in modern medical practices. Numerous drugs have been designed to exploit drug delivery systems, primarily oral administration, as it is preferred by the public for treatment of animals and humans. Butorphanol is a commonly used opioid analgesic drug for pain relief in avian species. The pharmacokinetic reports on butorphanol suggest that it is metabolised and cleared from an avian body at a much faster rate when compared to mammals. A single intravenous injection of butorphanol at 2 mg/kg provides analgesia for only 2 hours. When given at higher doses, butorphanol starts to produce side effects such as hyperventilation, cardiac insufficiency, coma and death. Therefore, there is a need to develop a slow release drug delivery system for butorphanol which can prolong the duration of analgesia without the side effects. Hydrogels are an emerging drug delivery strategy which can release drugs at a controlled rate and overcome many of the problems with traditional delivery techniques. This controlled delivery is vital for prolonged delivery of drugs which can be hazardous when applied in higher doses such as butorphanol. However, many modern hydrogels lack the stability for prolonged drug release or present other problems including prohibitive cost and bio-incompatibility. In order to solve these problems and improve the delivery system, hydrogels were developed using nanocellulose derivatives coupled with traditional hydrogel materials. These systems allowed slow sustained release of butorphanol in broiler chickens species with limited observed side effects due to the biocompatible nature of the hydrogels. The hydrogels provided an analgesic effect for up to 26.5 hours which was a longer time than the 4 hours produced by the subcutaneously injected commercially available butorphanol.

2. Literature review

2.1 Nanocellulose

2.1.1 Nanocellulose forms

Cellulose is a linear chain polysaccharide composed of multiple β -(1,4)-glycosidic linked D-glucose units⁹, and is an important structural component of the cell walls in algae, bacteria fungi, tunicates and plants. It can only be digested naturally by ruminants with specialised symbiotic microorganisms present in the gastrointestinal tract, specifically the rumen capable of breaking down the cellulose via fermentation reactions.

In recent years, interest in nanocellulose has increased due to its biocompatibility associated with its similarity to the human extracellular matrix, biodegradability and stability. In addition, its ability to form hydrogels and be chemically modified makes it an ideal material for use in biomedical applications. The two primary sources of nanocellulose are from plant matter such as wood pulp, cotton or hemp fibres (Fig 1), and bacterial sources such as *Gluconacetobacter xylinus* (*G. xylinus*).



Figure 1: Untreated hemp fibres.

There are three primary forms of nanocellulose currently being investigated: cellulose nanofibrils (CNF), cellulose nanocrystals (CNC) and bacterial nanocellulose BNC. CNF is extracted from wood pulp. It has a strong tensile strength, is capable of forming hydrogels and is currently used as a stabilising agent for food product. CNC is produced by acid treatment of native cellulose, preserving the crystalline areas, resulting in rod-like structures with a high specific strength. They are useful for mechanical stability and drug delivery systems. BNC is primarily produced by *G. xylinus*. It has a high tensile strength and a hydrophilic surface making it useful for drug delivery systems and tissue scaffolding for tissue engineering.¹⁰ Images of these three forms are shown in Figure 2.

Figure 2: Images of CNF (a), CNC (b) viewed by transmission electron microscopy and BNC (c) viewed via scanning electron microscopy.¹⁰ a shows the CNF units with 1-3 μm length and 2-60 nm width. b shows CNC with 10-50nm width and 100-500 nm length⁹. c shows BNC with 5-70 nm width and 100 nm length.¹¹ The weblike structure of the CNF and BNC and the rod-like structure of the BNC influence their binding characteristics.

The bulk of the literature currently available on nanocellulose hydrogels and their biomedical applications has focused on using the nanocellulose as a biological scaffold and/or drug delivery system for wound treatment due to its biocompatibility and mechanical properties.¹²

While many papers have shown the potential of nanocellulose hydrogels as drug delivery systems, few have produced complexes capable of releasing the drugs with a steady release rate using opioids, and even fewer studied for the use of hydrogel subcutaneous drug delivery systems in avian animal models.

2.1.2 Cellulose nanocrystals

Cellulose nanocrystals are prepared from woody materials such as cotton or hemp fibres. The fibres are then degraded using chemical or mechanical treatments (collectively called the top down approach) where the large quantity of starting material is sequentially broken down to remove waste material such as ligands and lipids.

The mechanical processes can involve high pressure homogenisation, high powered sonication and micro fluidisation techniques in order to apply shear stresses to the cellulose fibres, splitting them along the longitudinal axis in order to produce strings of cellulose crystals with disordered crystalline regions acting as linkages.

Chemical processes such as acid hydrolysis transform microfibrils of cellulose into crystalline nanocellulose with lower energy requirements than the mechanical treatments which produce short nanocrystals with improved crystallinity. The acid hydrolysis method uses strong acids to destroy the amorphous domains of the microfibrils while preserving the ordered crystalline sections.

Once the monocrystalline cellulose is isolated it can then be further modified to produce multiple forms of the rigid rod-like cellulose nanocrystals which possess many important properties such as high strength modulus, a large surface area and unique liquid crystalline properties.¹³

Nanocrystals are less suitable for drug delivering hydrogels than cellulose nanofibrils and bionanocellulose. This is due to the more rigid structure producing weaker 3D matrices that are potentially useful for developing flexible electronics displays and advanced battery systems.

2.1.3 Nanofibrillated cellulose

The primary form of nanocellulose produced by the top down approach is nanofibrillated cellulose from plant matter via mechanical or chemical treatments similar to those described in 2.1.4 in order to produce a 3D matrix of flexible and entangled chains of cellulose units. The properties do however differ from the other forms of nanocellulose by possessing a low gas permeability rate and a higher tensile strength allowing for a wide range of potential applications.

The material can then be further processed with chemical modifications for a wider variety of applications ranging from topical application of antibiotic drugs for wound treatment through to producing paper with improved sheet tensile properties.

2.1.4 TEMPO oxidation

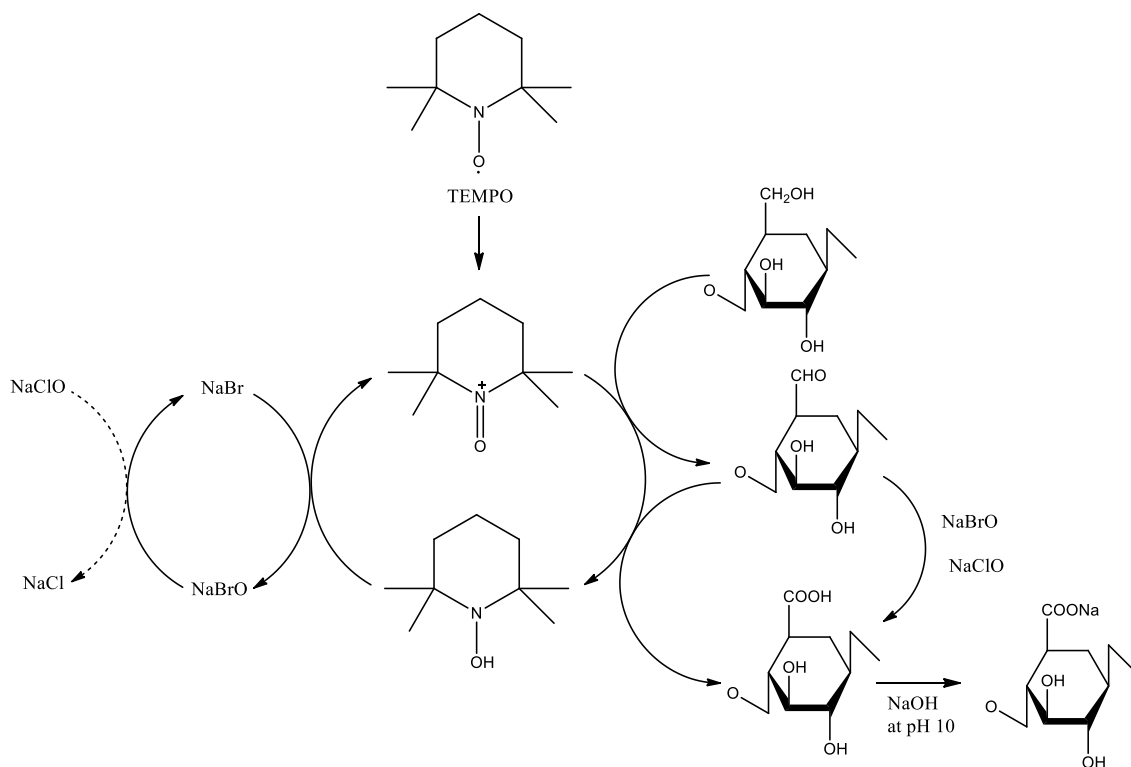


Figure 3: TEMPO oxidation of a primary alcohol to a carboxylic acid with a TEMPO catalyst, NaClO and NaBr suspended in water at pH 10.⁷

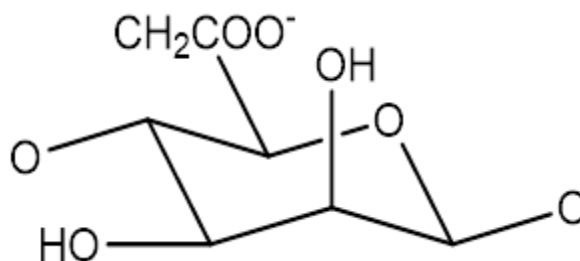


Figure 4: TEMPO oxidised cellulose monomer.

TEMPO oxidation (Fig 3) is a potential technique for the extraction and modification of nanofibrilated cellulose using chemical treatment of cellulose microfibrils to add negative charged entities to the fibre surface. 2,2,6,6-Tetramethylpiperidine-1-oxyl (TEMPO) is a highly stable catalyst which uses NaClO and NaBr to oxidise the primary alcohol groups on the cellulose fibres in order to produce carboxylate groups (COO⁻) in aqueous solutions with a primary oxidising agent (NaClO). The reaction is carried out at pH \approx 10 which leaves a small percentage of aldehyde groups which have not been completely oxidised to form the carboxylate groups.¹⁴

The COO⁻ groups provide a negative charge to the surface of the nanofibrillated cellulose (Fig 4) making the formation of ionic bonds possible by cross linking molecules such as Ca²⁺ with other negatively charged particles such as the carboxyl groups on sodium alginate and or chitosan that has an overall cationic charge.¹⁵

2.1.5 Bionanocellulose

Bionanocellulose is a form of nanocellulose produced primarily by the bacterial species *G. xylinus*. This species is a rod shaped, gram negative and an obligate aerobe which metabolises sugars, primarily glucose, to synthesise cellulose.

Figure 5: Potential biosynthesis pathway for cellulose production.⁴

Biosynthesis of the microbial cellulose occurs in the space between the outer wall and plasma membrane of the bacterial cells via bio-catalytic action of an enzymatic complex cellulose synthase with uridine diphosphate glucose (UDP-glucose) as the starting material. The UDP-glucose units are attached to polymeric chains with the reaction catalysed by the cellulose synthase.

This reaction has a high turnover rate with a single bacterial cell capable of converting greater than 100 glucose molecules into cellulose per hour¹⁶. This reaction is believed to follow the potential biosynthesis pathway (Fig 5).

Bionanocellulose is secreted by the bacterial species as an extracellular primary metabolite composed of cellulose microfibrils with nano metric widths thereby classing it as a nanomaterial due to one of the dimensions possessing a nano level order of magnitude.¹⁷

This nanocellulose is considered to be of higher quality than those produced by the breakdown of the complex plant matter via the top down approach, despite having the same molecular formulae. The bionanocellulose forms dense interconnected networks of cellulose chains capable of forming more absorbent and stronger hydrogels. Due to their more intricate structure with stronger and larger fibres, the strength of the crosslinking and the absorption coefficient are both increased.¹⁷

The limiting factors include the high unit cost, slow growth rates of the bacterium, current lack of large scale production facilities and the time intensive processing steps required, for example the Cross-Bayer reagent treatment of the cellulose pellicle takes multiple days in order to purify the nanocellulose.

2.2 Nanocellulose based hydrogels for avian analgesic drug delivery

Modern strategies for drug delivery present a balancing act between the release rate, efficiency and safety of the delivery strategy in question. Multiple factors need to be considered based upon the drug in question and the vector of administration.

There are three primary admission vectors for the introduction of drugs into a system: 1. the enteral route encompassing oral administration through the gastrointestinal tract (GIT), 2. per-rectal administration and 3. the parenteral route encompassing intramuscular, intravenous, intranasal, subcutaneous administration and topical application.¹⁸

2.3 Enteral routes

2.3.1 Oral administration

The oral route is the most common method for administering drugs to animals and humans due to its lower costs, the safety of delivery and the ease by which it can be applied. This route also presents limitations for the type of drugs available for delivery due to the wide pH range the drug must tolerate and the limited exposure time in the gastrointestinal tract where uptake is possible. There is also a decreased efficiency due to the presence of protecting components and slow uptake making this route impractical for rapid administration. Finally, there is a limited amount of drug reaching the desired tissue target, due to the initial passage through the liver (also called the *first-pass effect*).

2.3.2 Rectal administration

This is a route used for unresponsive or uncooperative patients where oral administration is not feasible. This route also bypasses the gastric acids present in the stomach, the lipases and carbohydrates present in saliva, thereby removing design constraints on the nature of the drug administration. The disadvantages are primarily around customer acceptance and the increased influence of the *first-pass effect* decreasing the amount of drug reaching the portal blood and then entering circulation.

2.3.3 Sub-lingual and buccal administration

This route involves the placing of pills beneath the tongue or in the cheek sulcus allowing rapid adsorption of the drug while simultaneously decreasing the *first-pass effect* by rapidly crossing the membrane barriers to enter the blood stream. The inconvenience to the patient involves the risk of swallowing and therefore removing the drug, with the added risk of irritation to the mucosal tissue prevents this drug delivery route from being widely accepted.

2.4 Parenteral routes

Parenteral is derived from the words 'para' meaning to bypass and 'enteron' meaning the alimentary canal between the mouth and the anus.

2.4.1 Subcutaneous injection

Subcutaneous injections introduce the drug between the skin and muscle layers using a short needle, as shown in Figure 6. This technique allows drugs to be delivered which would be substantially degraded by gastric acid or enzyme activity when administered orally to the patient. This type of injection allows for a slower release rate of the drug when compared to intramuscular injections due to the decreased blood flow rate in the area reducing the speed of the uptake rate of the drug into the circulatory system. The injection sites are primarily the upper arm, front of the thigh and lower abdominal area where there is a more accessible adipose layer. This strategy is commonly used to administer insulin.¹⁹

Figure 6: Subcutaneous injection technique.²

2.4.2 Intravenous injection

Intravenous injections are the most common parenteral route used by healthcare professionals, the drug is administered to the circulatory system immediately and adsorbed rapidly with dependable and replicable results. This also bypasses the *first-pass effect* on the drug's concentration within the system. However, this route can require cannulation of a vein which is problematic when patients have small veins. It is in many cases more expensive, labour intensive and potentially traumatic while providing an avenue for infection and the potential for an inflammatory response.²⁰

2.4.3 Intramuscular injections

For intramuscular injection, the drug is administered to deltoid, vastus lateralis, ventrogluteal or dorsogluteal muscles, as shown in Figure 7. This is dependent on the nature of administration (self-administration or by a healthcare provider), the size of the patient (infant, child, adult) and the nature of the drug being delivered (viscosity and volume).

Intramuscular injections are commonly used as a parenteral drug delivery route for application of slow release drugs, the tissue slowly releases the drug into the blood stream where it is absorbed and then there is rapid onset, a high absorption rate and the potential for oily materials to be used.

Figure 7: Intramuscular injection to deltoid.³

This technique is useful for infants where intravenous delivery is not practical, or for patients with collapsed or constricted veins such as habitual intravenous drug users or patients undergoing courses of chemotherapy.²⁰

2.4.4 Topical application

This route involves absorption of the drug through the skin layers in order to treat surface wounds, desensitise the skin or apply protection to the outer skin layers. This method is limited in application but is beneficial for treatment of wounds on extremities and can provide a mechanism to prevent infection and damage to the internal system. This is generally a slow uptake mechanism but is also widely acceptable to the public and does not require trained personnel for application such as diclofenac muscle/osteoarthritic gels.²¹

2.4.5 Intranasal application

This mechanism is a painless and simple application method which utilises the close proximity of the nose-brain pathway in order to deliver the drug rapidly to the cerebrospinal fluid. This is especially important for opioid delivery as the opioid receptors in the brain and spinal cord are responsible for the analgesic effect. The drugs also bypass the *first-pass effect* of the enteral routes minimising the breakdown of the drug. However, there are a limited number of drugs which can be applied this way due to the aerosol nature of the delivery and the high drug concentration required for an effective dose.²²

2.4.6 Blood-brain barrier

The Blood-Brain Barrier (BBB) is a key consideration when determining the delivery mechanism for opioids and other compounds that require access to the cerebral tissue to function. The BBB is the semipermeable membrane between the circulatory system and the cerebrospinal fluid present around the brain. This barrier is selective and limits the passage of microorganisms and large molecules based upon the water-levels,

polarity and the nature of the receptors bound to the drug membranes. Figure 8: Three strategies (A, B, C) for drug delivery through the BBB.¹

This is important for delivery of analgesics as they require access to the brain in order to function, if the drug cannot pass through the BBB it cannot function. If the BBB allows a limited amount of drug to pass slowly then the amount of drug that effects the brain will be drastically reduced.

There are a few strategies (Fig 8) that have been developed to deliver drugs through the BBB where they would normally be blocked. These strategies can disrupt the BBB itself, allowing passage of wanted and unwanted materials through (Fig 8A). Other strategies involve combining the therapeutic drug to another compound that can carry the drug through the BBB (Fig 8B) or bind to receptors for transport (Fig 8C) without compromising the barrier.¹

2.5 Traditional hydrogel materials

2.5.1 Alginate

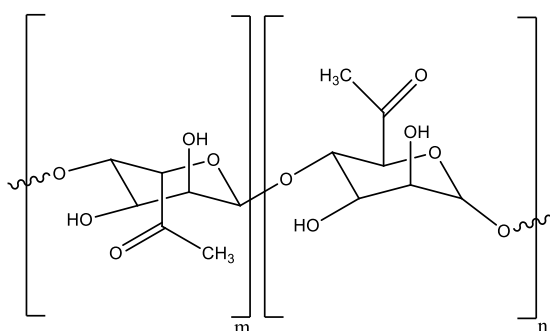


Figure 9: Alginic acid.

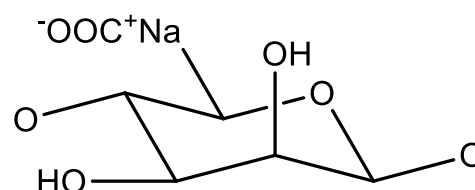


Figure 10: Sodium alginate monomer.

Alginate is the collective name for the group of naturally occurring anionic polysaccharides which have been extracted from brown algae strains (Fig 9). These include *Ascophyllum nodosum*, *Laminaria hyperborean*, *Macrocystis pyrifera* and the bacterial species *Azotobacter* and *pseudomonas*.²³

Sodium alginate (Fig 10) is composed of alginic acid with its sodium salt extracted from brown algae belonging to the Phaeophyceae phylum. It is also produced by the opportunistic bacterium *Pseudomonas aeruginosa* where it composes a large amount of the biofilm produced to confer resistance to antibiotics and destruction by macrophages. The survival of the *Pseudomonas* biofilm within a human system can lead to the development of cystic fibrosis when the immune system is compromised due to previous conditions or other diseases present.

The alginic acid component is composed of a co-polymer of homopolymeric blocks (Fig 9). These are (1-4)-linked β -D-mannuronate (m) and C-5 epimer α -L-guluronate (n) residues which can then be covalently linked together to form various sequences. The monomers can be present as blocks composed of consecutive m residues, n residues or a mixture of n and m residues. The ability of the co-polymer chains to absorb water into the matrix has led to sodium alginate being incorporated into multiple industrial applications including food, cosmetic and pharmaceutical.

2.5.2 Chitosan

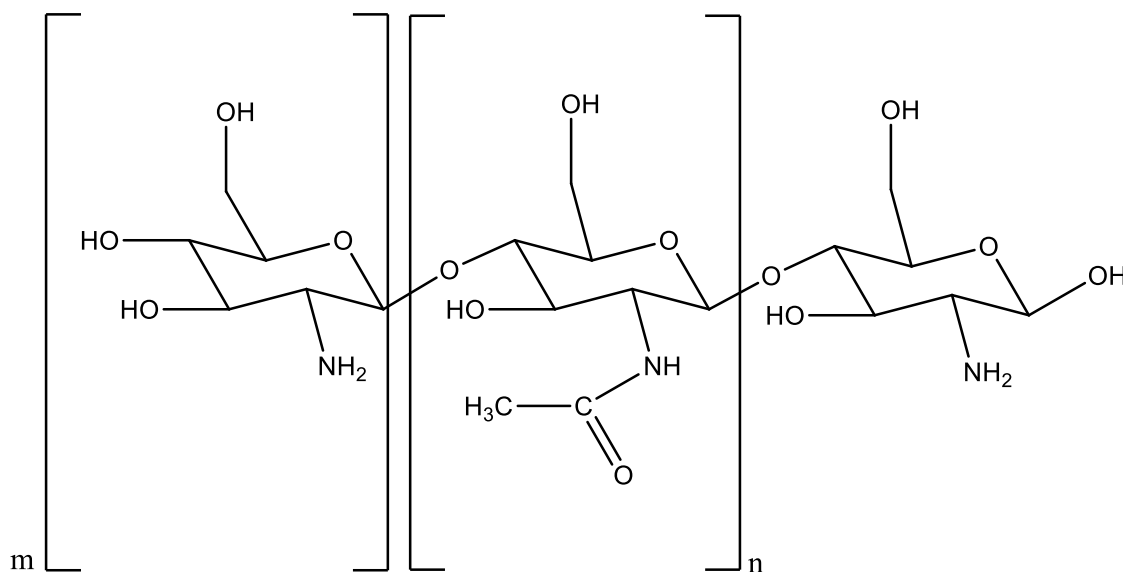


Figure 11: Deacetylated chitosan structure composed of deacetylated β -(1 \rightarrow 4) linked D-glucosamine (m) and acetylated N -acetyl-D-glucosamine (n).

Chitosan is a linear polysaccharide produced from chitin that had been treated with alkaline substances for deacetylation of the chitin. The linear polysaccharide is composed of the deacetylated β -(1 \rightarrow 4) linked D-glucosamine (m) and acetylated N -acetyl-D-glucosamine (n) randomly assembled together (Fig 11).

The original chitin is harvested from the shells of crustacean species. The shells are processed to isolate the pure chitin from the other biological materials. This process has garnered considerable appeal due to the wide availability of crustacean's shells which are a waste product from the seafood industry. This reduces the cost of the raw material and does not require new production facilities to produce the amounts required for commercial production. Japan is the primary producer of chitin and chitosan products with > 100 billion tonnes produced each year accounting for 90% of the global market.²⁴

The chitin is then further processed to form chitosan with the acetamido group turned into amino groups (Fig 12) allowing the chitosan to become soluble in water. There are two general processes to convert chitin to chitosan. A thermochemical based reaction and a biological based reaction using the enzyme, chitosan dehydrogenase.

One chemical procedure²⁵ involves demineralisation, deprotonation and deacetylation of the chitin. The demineralisation step involves prolonged treatment (16 hr) with HCl at ambient temperature (28°C) to remove any unwanted mineral components of the chitin. The second step is deprotonation which uses NaOH (20 hr) at ambient temperature (28°C) to remove any excess protons that may disrupt the deacetylation step.

The processed chitin is then dried and mechanically degraded to maximise the surface area. At this stage pure chitin has been produced. The deacetylation step is the final step with the pure chitin treated with NaOH at 65°C for 20 hr to produce chitosan.

The biological process involves using enzyme chitin deacetylase which catalyses the reaction of chitin with water to produce chitosan and acetate (Fig 12). The chitin deacetylase is not inhibited by the production of acetate so is not a self-limiting reaction.

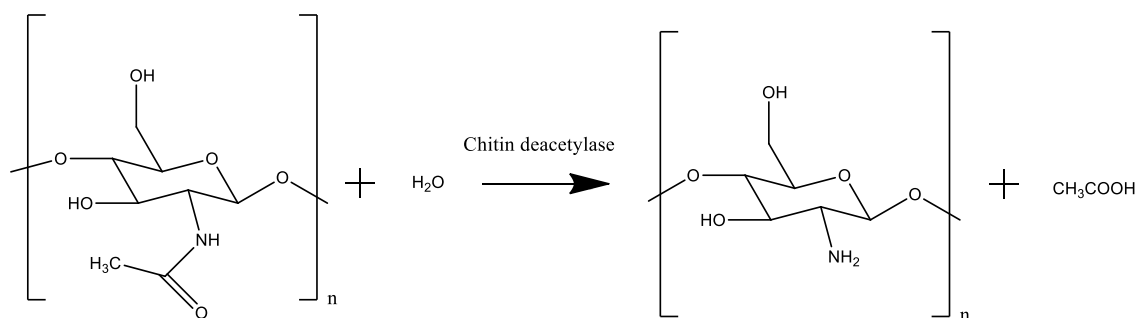


Figure 12: Chitin deacetylated to form chitosan and acetate with the catalyst chitin deacetylase.

This chemical process requires the use of non-recyclable chemicals and increased temperatures to produce the chitosan. The variables in production, such as species of crustacean used and difficulties controlling the temperature can lead to large variations in the chitosan produced. The biological process uses the enzyme chitin deacetylase and water with no additional chemical requirements and a lower ideal temperature of 50 °C.

Chitin solubility is determined by the percentage of deacetylation and the pH of the solution. Chitosan with lower levels of deacetylation ($\approx 40\%$) is soluble in solutions with a pH up to 9 and has a lower viscosity.

Chitosan with higher levels of deacetylation required lower pH solutions (up to 6.5) to remain soluble and has a higher viscosity. The viscosity is also increased with lower temperatures.

Increases in the chitosan concentration of the solution can also affect the viscosity of the solution at the same temperature.

The viscosity is affected by the degree of deacetylation due to the conformation of the molecule changing: with higher levels of deacetylated chitosan possessing, highly charged molecules form a flexible chain structure. Lower levels of deacetylation produce a lower charged compound with a rod-like structure.²⁶

2.6 Hydrogel drug delivery

2.6.1 Hydrogels

Hydrogels are a 3D network of polymer chains forming a hydrophilic complex. These can be crosslinked via covalent and/or ionic bonding, van der Waals forces or hydrogen bonding. Then stabilisation can occur by physical interactions such as electrostatic interactions, hydrophobic reactions and entanglement of the polymer chains.

A distinguishing trait of the hydrogels is their ability to absorb water, swelling the gel, extending the distance between the polymer chains while still maintaining the structural integrity. This contrasts with soluble gel materials which disperse into the liquid phase.

Hydrogel characteristics are dependent on the desired nature of the crosslinking reactions and the final properties of the hydrogel. In turn these characteristics are governed by the chemical modification of the polymer chains used to promote discrete binding patterns.

There are numerous polymers currently used to produce hydrogels. The most common polymers used are alginate and chitosan as they are affordable, biocompatible and have renewable sources. However there are many other natural polymers used including dextran, hyaluronic acid, nanocellulose and xanthan as well as synthetic polymers.²⁷

The swelling nature of the hydrogels and their capacity for large scale water uptake make it possible to use hydrogels as drug delivery systems for water soluble drugs including non-steroidal anti-inflammatory drugs (NSAIDs) and opioids such as butorphanol while maintaining the hydrogel systems structural integrity.²⁸

Hydrogels are currently used industrially for production of products ranging from contact lenses, advanced wound dressings, scaffolds for tissue engineering and disposable diapers. All of these products exploit the natural properties of the gels which include biodegradability and renewability of the starting materials.²⁹

2.6.1.1 Chemical crosslinking

One of the possible crosslinking reactions between monomers or polymer chains is a chemical crosslink which involves the sharing of electrons between the macromolecules. This crosslinking reaction involves the formation of covalent or ionic bonds which can change the physical properties of the hydrogel by introducing stronger bonds, which in turn creates a denser hydrogel and/or introduces crystallinity into the structure.³⁰ The melting point, solubility and viscosity can also be altered by varying the degree of crosslinking.

Crystallinity can increase the rigidity of the structure, decreasing its elasticity with the associated risk of making the gel brittle. The less elastic the gel, the more susceptible it is to shear stress which can damage or rupture the gel matrix causing a rapid release of any enclosed drug. However, the increased crystallinity also increases the melting point of the gel allowing a wider range of polymer chains to be used in hydrogel formation.

The viscosity of the gel can make the gel impractical for use in injectable solutions or topical creams. The flexibility between the polymer chains is required for the gel to be delivered via injections or placed upon fragile tissue, such as burns, without causing damage. This decrease in fluidity is caused by the crosslinking restricting the movement of the polymer

The increase in crosslinking will also decrease the solubility of the gel. With more crosslinks, the polymer chain binding increases and the gel becomes capable of taking up solvents without disrupting the gel matrix.

Ionic interactions involve the formation of an ionic bond between two species. This normally involves binding polymer chains together through a bridging ligand such as calcium ions which can bridge two negatively charged groups located on the polymers (Fig 13). This bridging forms bonds by the interaction of the negatively charged COO^- group with the positively charged Ca^{2+} ion.

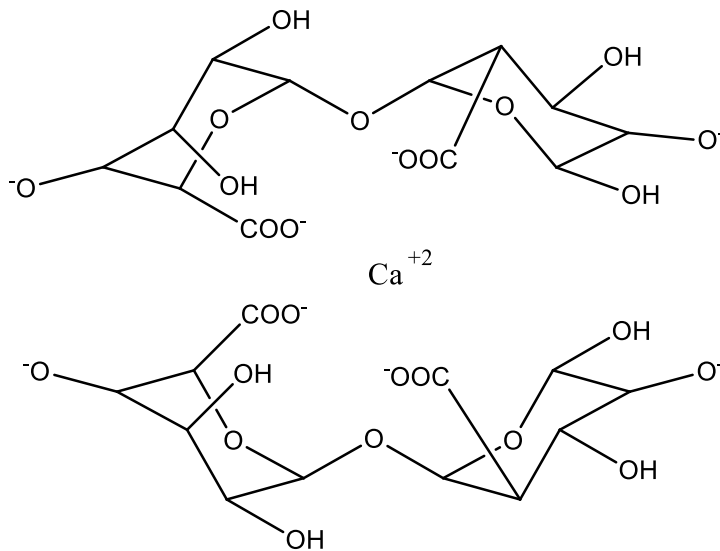


Figure 13: Sodium alginate crosslinked with calcium chloride to form ionic bonding.

These bonds are generally stronger and have a non-reversible nature making them ideal for producing hydrogels capable of maintaining their structure when placed under mechanical stresses. This is ideal for use in products such as wound dressings or artificial cartilage where the movement of the patient would degrade weaker gels.

A common chemical crosslinking reaction used in the formation of hydrogels is the Schiff Base reaction.³¹ This reaction involves the use of an imine to form crosslinking reactions between water soluble polymers to form insoluble hydrogels capable of absorbing water.

2.6.1.2 Physical crosslinking

Physical crosslinking involves the use of non-covalent bonding to form gel structures from polymer chains without forming covalent bonds. These gels can be formed via electrostatic interactions, hydrogen bonding, hydrophobic interactions or van der Waals forces.

Electrostatic interactions occur when the positively charged groups on one polymer chain is attracted to the negatively charged group present upon another polymer chain without creating a constant bond.

Hydrogen bonding can occur with the hydrogen atoms of one polymer being attracted to an electronegative atom present within the other polymer, this forms a strong bond to stabilise the hydrogel polymer (Fig 14).

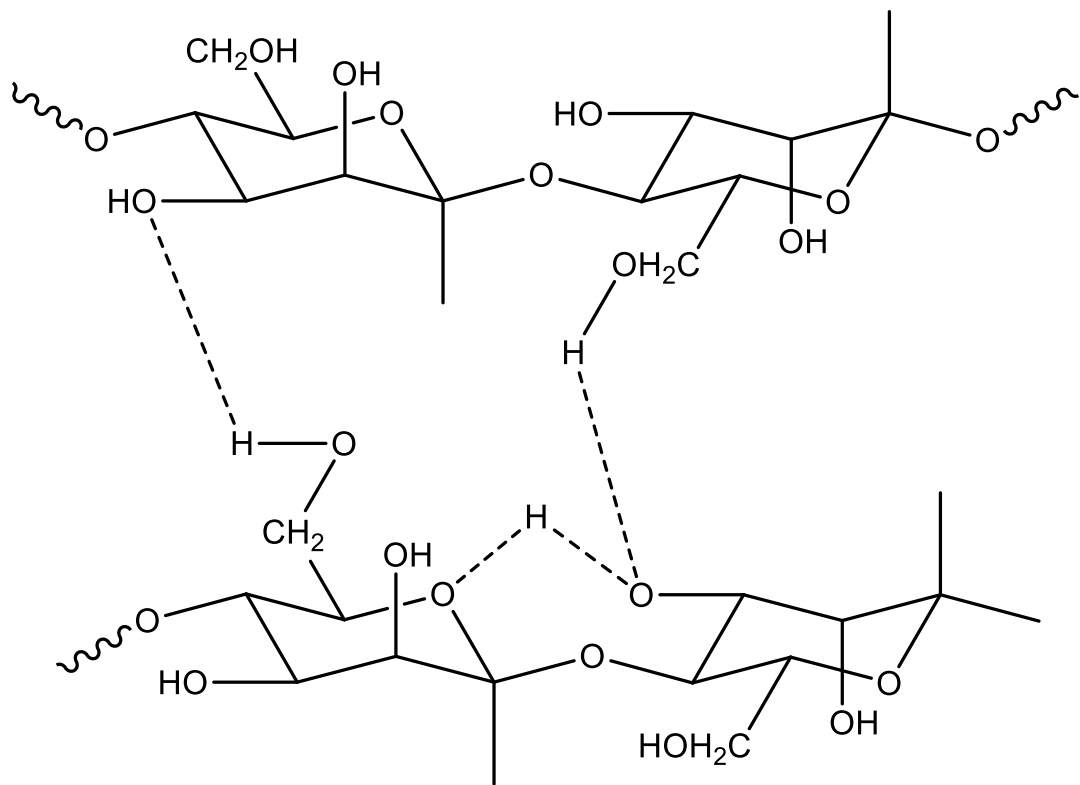


Figure 14: Hydrogen bonding between sodium alginate polymer chains.

Hydrophobic interactions can also promote gel formation when the polymers are repelled by the polar water which causes the polymers to condense into a gel structure.

Van der Waals forces are the sum of attractive and repulsive interactions between the polymer chains. If the attractive forces are stronger a bond can form. If enough of these bonds are formed a gel structure can result but the distance between the polymers is maintained as the closer the polymer chains become the stronger the repulsive force becomes.

These bonds can form naturally between the polymer chains forming a hydrogel or can be induced by altering the charge, pH, temperature or water content of the polymer solution.

The nature of these gels is normally characterised by a lower mechanical strength caused by the reversible nature of the non-covalent bonds. This can be exploited to produce hydrogels that can rapidly degrade, releasing any entrapped drug into the surrounding area allowing for targeted release when exposed to different conditions which break the bonds.

2.6.1.3 Hydrogel classification

Hydrogels can be classified based upon their composition, the nature of the crosslinking, the physical structure of the polymer chains and the charge of the monomers/polymers. These all affect the physical properties of the hydrogel and can change the hydrogels response to external stimuli such as pH, salt content or heat.

The hydrogel can be composed of natural or synthetic monomers or polymers. If there is only one form of polymer present it is a homo-polymeric hydrogel, if there are two distinct forms of polymer present it is classed as a co-polymeric hydrogel. If there are two or more polymer networks fully interlaced without forming covalent bonds, the hydrogel is referred to as an interpenetrating polymer network. If there are two or more polymer networks that are at least partially interlaced without the formation of covalent bonds, the hydrogel is referred to as a semi-interpenetrating polymer network (semi-IPN). If the networks are not interlaced at all the hydrogel is referred to as a polymeric blend.

The crosslinking can be either chemical or physical: chemical crosslinking producing stronger bonds that are non-reversible; physical crosslinking which has weaker, reversible bonds.

The physical structure of the hydrogel can be *amorphous* where the chains are randomly positioned with no crystallinity present, *semi-crystalline* where there are regions of the hydrogel containing partially ordered sections and *hydrogen-bound* where there are hydrogen bonds between the polymers in the gel forming a stable network.

The charges on the monomer/polymer can influence the electrostatic interactions between regions with alternate charges (positive to negative and vice versa) and the chemical bonding to crosslinking agents. These can change the overall charge of the hydrogel to negative where it is described as an *anionic* gel, no charge where it is neutral, positively charged where it is called *cationic* and when the gel charge contains both positive and negative sections it is called and *amphipathic* hydrogel.

2.6.1.4 Smart hydrogels

Smart hydrogels are classified as hydrogels that respond to external stimuli, altering the swelling behaviours of the hydrogel. This can be exploited to produce gels which can specifically target certain areas such as the lower intestine while being capable of passing through the low pH stomach without releasing an encapsulated drug.

This form of hydrogel is considered to be a potential future in drug delivery due to its selective nature. An example of this has been to produce a gel which selectively releases an encapsulate drug when exposed to UV light. The UV light promotes protonation, this protonation then alters the pH allowing for the rapid release of an encapsulated drug in the illuminated areas directly and in the non-illuminated areas through proton transfer.³²

2.6.2 Opioids

Opioids or opiates are a class of drugs that reversibly bind to the opioid receptors located within both central nervous system and periphery^{33,33a}. The opioids affect the system by mimicking three endogenous peptide endorphins which are found naturally within the body. The three peptides are β -endorphins, enkephalins and dynorphins. These peptides then bind to the opioid receptors to produce an effect similar to morphine by reducing the sensation of pain.³⁴

The opioid receptors in the central nervous system are divided into three main subgroups; mu (μ), kappa (κ), and delta (δ) depending on the corresponding endogenous peptides. When bound, the drug can be displaced by the μ -opioid receptor antagonist naloxone.³⁵

Administration of naloxone is therefore commonly used to rapidly treat overdoses of opioids and reduce or remove the associated effects including excessive drowsiness, slowed breathing and loss of consciousness.³⁶ Opiates are extracted from opium poppy *Papaver somniferum* originally from the eastern Mediterranean. The main use of these opioid alkaloids is as an analgesic for medical and veterinary practices despite the addictive properties.

The opiates can be applied via the intramuscular, intravenous, oral, rectal, and nasal routes dependent on the nature of the opioid, the desired effect and the capabilities of the person administering the drugs.

The person administering the drug is important as the various administration techniques require various levels of technical skill. For example, oral administration can be done by most of the general public but the ability to inject into a vein requires more specialised training to prevent damage to the veins or injection into an incorrect area.

The most commonly used opiates are morphine and codeine, which are natural alkaloids extracted from the opium poppy. Hydromorphone and oxycodone are examples of semi-synthetic opiates which have been derived from natural opiates.

Fully synthetic opioids such as pethidine and the fentanyl series, methadone and tramadol are also widely used.³⁷

2.6.2.1 Butorphanol

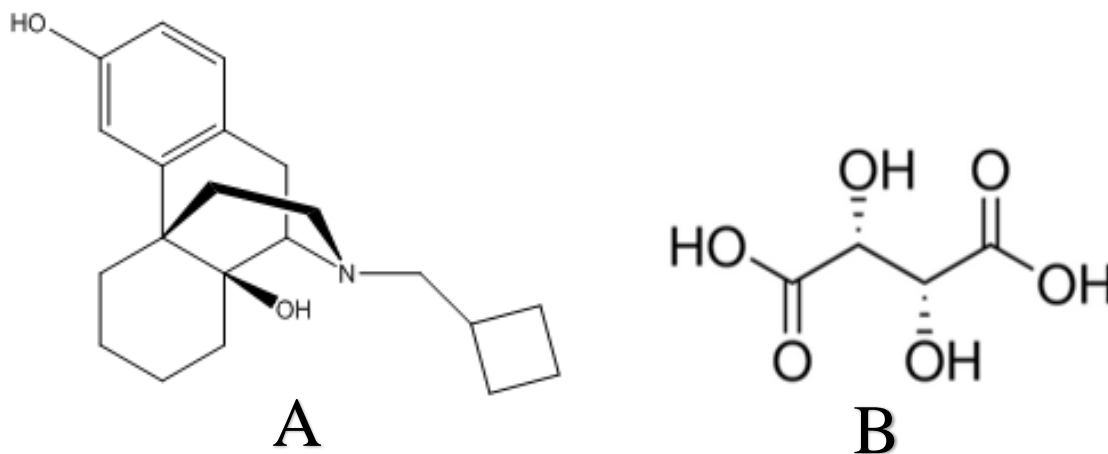


Figure 15: Chemical structure of butorphanol (A) with the peripheral tartrate ligand (B).

Butorphanol tartrate (Fig 15) is a highly hydrophilic synthetic opioid commonly used in veterinarian practice for relief of acute pain.³⁸ It can be administered by traditional oral and parental routes or in the nasal passage where it is rapidly absorbed and delivered to the active opioid receptors within the brain.

Butorphanol is a kappa receptor agonist and mu receptor antagonist.³⁸ In birds, butorphanol is thought to be effective as it is a κ receptor agonist and birds have a higher proportion of κ receptors compared with other species.³⁹

The central opioid receptors are divided into five main subgroups; δ , κ , μ , ζ and nociception receptors, depending on their effects. For example, the δ , κ , μ receptors are linked to the peripheral sensory neurons responsible for pain transmission.

The level of the primary opioid receptors, δ , κ , μ differ across the animal species. Examples of this are shown in Table 1.

The δ receptors are responsible for analgesic, antidepressant, convulsive and physical dependence effects. This physical dependence can cause dramatic withdrawal signs associated with opioid addiction when the opioid usage is reduced.

This means a slow withdrawing period of gradually decreasing opioid doses is required for safely ending a patient's treatment.

Table 1: Summary of δ , κ , μ receptor percentage ratios in multiple species.⁶

	μ	κ	δ
Frog brain	37%	19%	44%
Chicken forebrain	58%	25%	17%
Pidgeon brain	14%	76%	10%
Junco (passerive) brain	74%	22%	4%
Rat forebrain	41%	9%	50%
Mouse forebrain	25%	13%	62%
Guinea pig forebrain	25%	50%	25%
Dog cortex	5%	58%	37%
Human cortex	29%	37%	34%

The κ receptors are responsible for analgesic, anticonvulsive, sedative and stress effects. The μ receptors are split into 3 subsections: $\mu 1$ is responsible for the analgesic effect while also causing physical dependence; $\mu 2$ causes the majority of the detrimental effects including respiratory depression, the euphoric effect associated with addiction and the physical dependence; $\mu 3$ is responsible for vasodilation where the blood vessels are dilated, lowering the patient's blood pressure.

ζ and nociceptin receptors are not involved in analgesic effects and therefore are not a target of interest for this study.

One of the main concerns about opioids is when the effective dose requires a high concentration close to the lethal dose to be effective. Variations in patient metabolism can potentially lead to overdoses due to different tolerance levels and uptake rates.

Within a model mammalian species (mice), the dose that was lethal for 50% of the test sample, LD_{50} , for intravenous administration was found to be 40-57 mg/kg in mice and 17-20 mg/kg in rats while oral administration had LD_{50} rates of 395-572 mg/kg and 570-756 mg/kg respectively.³⁴

2.6.2.2 Avian drug delivery

One of the prominent differences between the mammalian analgesic effect and the avian analgesic effect relates to the types of opioid receptors in their brains. Avian species brains have a greater amount of κ receptors compared to the μ or δ receptors associated with the mammalian analgesic effect. This means that opioids used on mammalian species which possess high numbers of μ or δ receptors are less effective in avian species (Table 1). Opioids that are less effective in mammals, such as butorphanol, become more potent due to specific targeting with variation depending on the specific avian species.⁴⁰

Studies on pharmacokinetics of butorphanol in birds^{41,41b} show that butorphanol is metabolized faster in birds and requires slower release techniques, like mini osmotic pumps⁴², polyoxomer gel⁴³, liposomes.⁴⁴

Osmotic pumps are small cylindrical implants that do not require an energy source. They function by exploiting the osmotic effect, as the extracellular fluid of the patient diffuses through the outer semipermeable membrane the osmotic compartment expands. This puts pressure onto the inner flexible reservoir where the drug is present. The drug rate of release is caused by the osmotic agent instead of the concentration of the drug present. This can dramatically reduce the rate butorphanol is released, extending the time where the analgesic effect is present but also increases the time until the analgesic effect is produced (6-12 hr).⁴²

Polyoxomer gels are a thermally sensitive hydrogel that can be loaded with butorphanol and provide an analgesic effect for a longer period than the commercial solution. However the analgesic effect was only sustainable for 4-8 hrs.⁴³

Binding butorphanol to liposomes to form a liposomal formulation can also be used to provide an analgesic effect in avians for 72hr.⁴⁴

While these three delivery systems provide possible solutions for long term analgesic treatment using butorphanol, they all possess issues that may limit their application.

The osmotic pumps take a long time to produce an analgesic effect and must be surgically removed. The polyoxomer gel provides an analgesic effect for a longer time but is still not efficient for longer treatments. The liposomal formulation was effective but is not commercially available and requires powdered butorphanol tartrate for preparation.

2.6.3 Animal trials

2.6.3.1 Three R's

The key principles for ethical animal testing are replacement, reduction or refinement. The three R's were developed to minimise or remove the suffering of animals for experimental testing while still obtaining the required results.⁴⁵

Replacement can involve the use of an *absolute replacement*, such as using a cell line or computer program for testing instead of animal models or *relative replacement* focusing upon the sentient nature, rarity or response to pain.

With relative replacement, more developed vertebrates such as canines or primates are replaced with less developed or more common vertebrates such as chickens or rats. The replacement of vertebrate species with invertebrate species with fewer sensory receptors is also preferable as the discomfort to the animal can be minimised when the pain response is not required to be measured.

Reduction refers to reducing the number of animals required for the experiment while still producing sufficiently accurate results by maximising the amount of data obtained per animal or minimising the amount of animal replicates required to answer a scientific question.

Refinement focuses on the wellbeing and treatment of the animals instead of changing the animal type or number. By improving the living conditions, the distress and discomfort to the animal can be dramatically reduced. Examples of this include providing temperature controlled areas, abundant food and water sources with areas provided for exercise.

The three R's not only improve the conditions for the animals but can improve the public's perception of research involving animal testing and dispelling the pre-conceptions of animal cruelty present within society.

With the inadequate correlation between animal model responses and human responses the development of absolute replacements becomes more important, especially within the pharmaceutical industry. This is because the development process takes an average of 14 years from conception to approval and up to 95% of therapeutic drugs fail to make it onto the market.⁴⁶

If a therapeutic drug produces adverse reactions or decreased efficiency in animal models yet would be more effective in human models, it would be discarded as human trials require rigorous testing before they can be attempted. The development of a human analogue is far more desirable than the use of animal models in order to understand the effects the drugs may have.

2.7 Biocompatibility issues

2.7.1 Non-specific defences

Non-specific biochemical and physical interactions form the primary defence system that prevents or hinders foreign material entering the system. There are many non-specific defences such as the acidic environment in the stomach, phagocytes in the blood which engulf and, remove cellular debris, in addition to intact skin and nasal mucous which prevents foreign materials entering the system.

Also, there are lysozymes in the saliva which can break down bacterial cells before they reach the stomach and commensal bacteria in the gastrointestinal tract compete with foreign bacteria for space and nutrition. Finally, there is an increased temperature or fever which is the system's final effort to prevent the foreign microbes spreading.

This increased temperature moves the environment outside the microbe's optimal temperature range but may cause damage to the system and if not controlled can lead to death.

2.7.2 Inflammatory response

The inflammatory response is of particular concern when administering drugs subcutaneously as the response is designed to be triggered by foreign material in the system. The subsequent swelling and tissue damage makes certain materials unusable in delivery systems.

The inflammatory response is triggered by the Pattern Recognition Receptors (PRRs) on specific cellular components such as macrophages and mast cells. These receptors are triggered by cellular damage called Damage Associated Molecular Patterns (DAMPs) or invading microbes called Pathogen Associated Molecular Patterns (PAMPs). Ideally a substance used for drug administration will cause limited cellular damage reducing the amount of DAMPs produced and increasing the strength of the immune response.

Once the PRRs are triggered they attract various forms of leukocytes. These include neutrophils which are responsible for initiation and maintenance of the inflammation response and phagocytes which engulf foreign pathogens forming a phagosome. Phagosomes can merge with lysosomes triggering degradation of the engulfed pathogen through the release of oxidative species.

2.8 Industrial applications of nanocellulose and bionanocellulose

In recent years, there has been a drive towards producing renewable and environmentally friendly materials in the pharmaceutical industry. This has led to increased attention for materials traditionally considered impractical due to availability, cost or time requirements. One of the materials now receiving considerable attention is nanocellulose, specifically bionanocellulose which has been used in a variety of medical applications.

2.8.1 Nanoskin

Nanoskin is the term for an emerging treatment for chronic wounds and burns. Nanoskin utilises bionanocellulose to produce membranes for tissue scaffolding. It promotes autolytic debridement which is the painless removal of necrotic tissue via enzymatic degradation, reduction of pain and acceleration of granulation where lumpy tissue containing connective tissue and capillaries form. These are all important factors for the promotion of healthy and rapid wound healing.⁵

The main wounds that Nanoskin has been used to repair include lacerations or foot ulcers caused by diabetes mellitus and burned tissue. Traditionally these chronic wounds disrupt the normal wound healing process such as reduced production of growth factors, collagen accumulation and inhibiting granulation.⁴⁷

Figure 16: Wound treated with Nanoskin for 19 days.⁵

Other wounds include burns where the epidermal and dermal skin layers have been severely damaged, compromising the integrity of the dermal barrier. When the barrier is compromised there is a very high risk of bacterial infection. The Nanoskin increases the rate of wound healing by providing a scaffold for tissue growth and allowing the passage or imbedding of antibiotic agents within its porous material. This prevents infection of the wound while also reducing scar tissue formation (Fig 16).

2.8.2 Bone repair

Degradation and loss of bone structure caused by trauma, reconstructive surgery or congenital defects present considerable problems for the medical industry. Nanocellulose composites have already been shown to aid cellular growth for chronic wounds and the aim is to apply this theory to bone repair.

Current research into bone repair is primarily focused on proof of concept with few animal trials conducted. One of the *in vivo* animal tests did however show promising results. The promotion in bone growth involved growth of osteoblast cells, high levels of alkaline phosphatase activity and increased bone nodule formation.⁴⁸

2.8.3 Nanocellulose drug delivery systems

Cellulose has been used traditionally as an excipient in order to condense drug loaded matrices making oral administration possible as it is non-digestible in the human digestive system. It is also not swollen to a dramatic extent within the digestive tract and possesses strong binding properties allowing it to be attached to rapidly dissolving active drug compounds.⁴⁹

Currently there is ongoing research into micro and nanofibrillated cellulose which possess a higher purity and can be altered to change the binding characteristics. These factors make cellulose applicable for use as oral tablet excipients or a prolonged drug release system.⁴⁸ The swelling nature is also altered from the traditional cellulose excipient, for example CNCs are capable of swelling and have been used for uptake and delivery of water soluble antibiotics such as tetracycline.

The nanocellulose can also be used as a co-stabiliser with other excipients such as acrylic beads to improve physiochemical and flow properties. An example is the binding of CNC which improved the size and size distribution of the beads forming a stable structure with a low flow time. Another use is for spray drying treatment on tablets with CNF, enabling packing with lower powder porosity and increased mechanical properties.⁴⁸

2.8.4 Soft contact lenses

A hydrogel composed of poly(vinyl alcohol), a water soluble synthetic polymer, is used to produce soft contact lens that have a higher tensile strength and absorb fewer proteins from the eye than the traditional poly(2-hydroxyethyl methacrylate) lenses.⁵⁰

This creates a lens that causes less irritation to the eye and is less prone to damage, increasing the lifespan of the lens.

2.9 Non-medical industrial applications of hydrogels

2.9.1 Disposable nappies

Another commercial use of hydrogels focuses on the ability to absorb water rapidly and to retain large volumes of fluid. The production of a low-cost material that is highly absorbent and biodegradable made hydrogels composites ideal to be integrated with traditional fibres for use in nappies.

The fibres increased the absorption rate of fluid into the hydrogel with the hydrogel swelling and entrapping the fluid for ease of disposal.

2.10 Cellulose harvesting

Cellulose harvesting from hemp is done by separating the rough outer fibres from the hurd. The hurd is the cellulose core which contains a higher amount of the high quality cellulose material desired for nanocellulose production. This can be done through two separate processes, decortication or retting.

The traditional technique used to separate the rough fibres from the hurd is known as retting. Retting can be done as dry retting or wet retting. Wet retting is far more water intensive but produces higher quality hurd. Dry wetting relies on natural dew fall and produces lower quality hurd.⁵¹

The wet retting process involves submerging bundles of the hemp stalks in either still or slow-moving water sources such as creeks, ponds or within large vats. The water permeates the hemp stalks, making the inner plant cells swell, this applies pressure to the outer cells which causes them to rupture. The damaged outer fibres then become more susceptible to bacteria which are capable of degrading the cells. This damage makes the outer fibres easier to remove mechanically.

The dry retting process requires high dew fall, the stalks are bundled together and left exposed to the elements. Bacteria then degrade the stem material which surround the fibre bundles via fermentation. After retting the stalks are dried and then the woody part of the stem is broken mechanically and removed leaving the desired hurd.

2.11 Analytical techniques

2.11.1 Liquid chromatography

Liquid chromatography is a separation technique which has been used in a wide range of academic and industrial chemical practices. Its primary purpose is to separate components within a complex mixture, so that the components can then be analysed or extracted as the purified form. The separation is a result of interactions between the mixture, mobile and solid phase which determines the type of separation achieved.

The most common method is liquid-solid chromatography which has the mixture present in the mobile phase passing over a solid phase which binds to the compounds resulting in the desired separation.

The separation is dictated by the polarity of the mixture and the phases; this results in the various compounds migrating through the solid phase column at different rates. Each with its own retention time on the column.⁵²

2.11.2 Normal and reverse phase chromatography

Normal phase chromatography involves a mobile phase which is less polar than the solid phase (column), the components present in the mixture contain varying polarities and will therefore elute at different rates. This technique works most efficiently for non-polar compounds, the polar compounds in the mixture are attracted to the polar solid phase so have higher retention times. Non-polar molecules which have lower retention rates can then be eluted and analysed faster.

This requires less time, making it easier to analyse multiple samples within the same time period while also reducing the amount of mobile phase required.

Reverse phase chromatography is a similar form of chromatography that involves a solid phase (column) which is less polar than the mobile phase allowing separation of the more polar molecules with decreased retention times

2.11.3 High performance liquid chromatography (HPLC)

HPLC is a separation method based on the principles of liquid chromatography and can use normal or reverse phase columns but it also uses a high-pressure system to enhance the separation of molecules for collection and then analysis of the compounds using an ultraviolet or fluorescence detector.⁵³

The separation is achieved by a liquid solvent being passed through an absorbent solid phase which separates the individual components based upon their retention times for collection, identification or quantitation.

2.12 Project Aims

The literature review has shown that there are currently problems with the traditional drug delivery systems used for avian analgesia. While butorphanol is an effective analgesic, it is rapidly degraded within the body and only produces an analgesic effect for a limited time when intravenously injected. Higher dosages of butorphanol also have a chance to cause detrimental side effects which are not acceptable. The alternatives such as osmotic pumps all present alternative problems including surgical requirements and a long-time period between administration and the analgesic effect being achieved.

The literature has also shown that hydrogels presented an interesting avenue of research for producing a safe and effective delivery technique, especially when the hydrogel incorporates nanocellulose derivatives. These derivatives have been shown to increase the structural stability which is necessary for prolonged release.

This project aims to solve these problems by producing a hydrogel incorporating traditional hydrogel materials and nanocellulose derivatives that are then crosslinked together. The hydrogel will be capable of taking up analgesic drugs such as butorphanol and then releasing the drug at a slow controlled rate. The hydrogels will be examined with *in-vitro* analysis and *in-vivo* analysis using broiler chickens.

The *in-vitro* analysis will involve submerging the butorphanol loaded hydrogel into solution and measuring the concentration of butorphanol in the solution over set time points.

The *in-vivo* analysis will involve administering broiler chickens with the butorphanol loaded hydrogel and measuring the butorphanol levels of the serum at set time points. Commercial solutions of butorphanol will be administered to broiler chickens with the same dosage. The serum samples will then be analysed using HPLC to determine how much butorphanol is present in the serum at each time point and then extrapolated to reveal the release rate of the hydrogel.

3. Methodology

Materials and equipment

Chemicals:

Acetone (CH₃)₂CO, MWt: 58.08 gmol⁻¹, CAS 67-64-1, Analytical reagent grade ≥99.5%, Fischer Scientific UK

Acetonitrile CH₃CN, MWt 41.05 gmol⁻¹, 0.786 kgL⁻¹, CAS 75-05-8, HPLC analytical grade 99.8%, Sigma Aldrich NZ

Butorphanol tartrate C₂₁H₂₉NO₂, MWt 327.473, CAS 42408-82-2, Ethical Agents Ltd

Calcium carbonate CaCO₃, MWt 100.0869 gmol⁻¹, CAS 474-34-1, BDH Chemical Ltd Poole England

Calcium chloride CaCl₂, MWt 110.98 gmol⁻¹, CAS 10043-52-4, AJAX Finechem

Chitosan 75-85% Deacetylated, CAS 9012-76-4, Sigma-Aldrich NZ

Disodium hydrogen phosphate dihydrate Na₂HPO₄·2H₂O, MWt 177.99 gmol⁻¹, CAS 10028-24-7, BDH Chemical Ltd Poole England

Glucose C₆H₁₂O₆, MWt 180.156 gmol⁻¹, Merck

Heparin C₁₂H₁₉NO₂₀S₃, CAS 9005-49-6, ProVet NZ

Hydrochloric acid – concentrated Hydrochloric acid: HCl, MWt 36.46 gmol⁻¹, 1.2kgL⁻¹, 12.18M, CAS 7647-01-0. Sigma-Aldrich NZ.

Monosodium phosphate NaH₂PO₄, MWt 119.98 gmol⁻¹, CAS 7558-80-7, Honeywell Riedel-de Haen

Orthophosphoric acid – concentrated Orthophosphoric acid: H₃PO₄, MWt 97.994 gmol⁻¹, 7664-38-2, 14.8, AJAX Finechem

Sodium alginate (C₆H₈O₆)_n(Na)_n, extracted from brown algae, low viscosity, CAS 9005-38-3, Sigma-Aldrich NZ

Sodium bromide NaBr, MWt 102.90 gmol⁻¹, CAS 7647-15-6, BDH Chemical Ltd Poole England

Sodium chlorite NaClO₂, MWt 90.44 gmol⁻¹, CAS 7758-19-2, technical grade 80%, Sigma-Aldrich NZ

Sodium hydroxide NaOH, MWt 39.997 gmol⁻¹, CAS 1310-73-2 ACS, ISO. Scharlau

Sodium hypochlorite NaClO, MWt 74.44 gmol⁻¹, 42 gL⁻¹, CAS 7681-52-9, Sigma-Aldrich, NZ

TEMPO 2,2,6,6-Tetramethyl-1-piperidinyloxy: 98% C₉H₁₈NO, MWt 156.25 gmol⁻¹, CAS 2564-83-2, Sigma-Aldrich NZ

Equipment:

22 G catheter - 0.9 x 25 mm, 35 mL/min, BD Insyte

C18 reverse phase HPLC column Synergi 4µm Fusion – RP 80 Å, LC column 150 x 4.6mm, P/no OOF-4424-EO

SPE cartridges Phenomenex Strata-X 33µm, Polymetric Reversed Phase SPE cartridges, 10 mg/1 mL Phenomenex NZ

Yeast extract Yeast extract, extracted from autolysed yeast, Baco

Machinery:

Centrifuge Eppendorf® Refrigerated Microcentrifuge, Model 5417r

Freeze drier Non-volatile substances, Model 8891F-MT, John Morris Scientific Ltd

Homogeniser Model - PowerGen 125, Fischer Scientific

HPLC UFLC Shimadzu HPLC, Liquid chromatograph LC-20AD, Auto sampler SIL-20AC HT, Degasser DGU-20A₃, Column oven CTO-20A, Diode array detector SPD-M20A

Multi-tube vortex SMI multi tube vortex, Model 2601, Scientific Manufacturing Industries

pH meter Mettler Toledo, Model 220 pH Meter

Sonicator Model 8891F-MT, Cole-Parmer

Vacuum Drier Savant Model SC210A, Speed Vac Concentrator, 10 mPa, Thermo Scientific

Solutions:

Butorphanol standard curve Serial 10 fold 1 mL dilutions of commercial butorphanol tartrate (10 mg/mL) with mobile phase to produce 1 µg/mL then serial 2 fold 1 mL dilutions with mobile phase to produce 15.6 ng/mL. The concentrations used for the standard curve were: 1 µg/mL, 500 ng/mL, 250 ng/mL, 125 ng/mL, 62.5 ng/mL, 31.2 ng/mL, 15.6 ng/mL

GYC Media was prepared in RO H₂O, it was composed of 10% w/v glucose, 1% w/v yeast extract, 2% w/v CaCO₃ with the pH set to 6.8 and autoclaved.

Hydrochloric acid – diluted 1.015 molL⁻¹ dilute hydrochloric acid solution was prepared from 50 mL 12.18 molL⁻¹ stock hydrochloric acid diluted in 550 mL RO H₂O.

Hydrochloric acid - 2M 2.03 molL⁻¹ HCL was prepared from 50 mL 12.18 molL⁻¹ stock hydrochloric acid diluted in 250 mL RO H₂O

Mobile phase – pH 4 Mobile phase for RP-HPLC was prepared from 80% phosphate buffer and 20% acetonitrile which was then vortexed for 30 s

Orthophosphoric acid – Diluted 1.06 molL⁻¹ dilute orthophosphoric acid was prepared from 50mL 14.8 molL⁻¹ stock orthophosphoric acid diluted in 650 mL RO H₂O

Phosphate buffer Two solutions were prepared to produce the pH 4 phosphate buffer (0.1 M). A solution of Na₂HPO₄ (0.2 M) was prepared from 14.15 g Na₂HPO₄ salt dissolved in 500 mL RO H₂O and a solution of NaHPO₄ (0.2 M) was prepared from 11.99 g NaHPO₄ salt dissolved in 500 mL RO H₂O.

The phosphate buffer (0.1 M) was then prepared from 187.5 mL of the 0.2 M Na₂HPO₄ and 312.5 mL of the 0.2 M NaHPO₄ and made up to 1 L with RO H₂O in a 1 L Duran bottle. The pH was then set to 4 using 1 M ortho-phosphoric acid to lower the pH and 1 M NaOH solution to raise the solutions pH if overshoot. Care was taken to minimise the amount of NaOH required, this was done to limit its effect upon the HPLC column.

Sodium hydroxide – diluted 1 mg/mL NaOH was prepared from 40 g NaOH dissolved in 1 L RO H₂O

3.1 Nanocellulose preparation

3.1.1 Chemical preparation top down approach

To remove any waxy components, the initial hemp fibres were chemically treated with a 9:1 acetone:water mixture over 48 hrs. The mixture was then vacuum filtered, washed 4 times with 100 mL aliquots of RO H₂O, filtered again and dried in a 60°C oven.



Figure 17: Hemp fibres after NaClO₂ treatment.

To remove the ligand components, the dried treated fibres were stirred in a pH 5 solution composed of 0.6 g NaClO₂, 1g treated fibres with 32 mL of RO H₂O for every 1 g of solid material, the temperature was maintained at 70°C.

The aqueous solution of NaClO₂ was replaced every 3 hrs with a fresh solution. The solid material was filtered off and then added to a new volume of solution at the same temperature.

After 15 hrs the fibres were then filtered and washed with 100 mL of RO H₂O 4 times, blended in a commercial blender on high speed, re-filtered and freeze dried. The processed fibres produced had a pale yellow/white colour with a soft texture similar to cotton fibres (Fig 17).

3.1.2 Biological preparation

This preparation strategy focused upon exploiting the bacterium *G. xylinus* in order to produce high quality nanocellulose which was required for medical purposes.



Figure 18: Cellulose pellicle produced by *G. xylinus* in GYC media.

The initial colonies of *G. xylinus* were taken off a GYC agar plate, supplied by the Institute of Fundamental Sciences, and used to incubate a 10 mL culture of GYC media within a test tube with a cotton wool plug.

The culture was then incubated at 30°C for 48 hrs, during this time it produced a cellulose pellicle. The test tube culture was then used to inoculate 200 mL of GYC medium in a 500 mL Duran bottle and was re-incubated for a further 48 hrs.

The culture was then removed and placed into a 2 L Erlenmeyer flask containing 1 L of GYC media and re-incubated for 6 weeks where it produced a thick pellicle of nanocellulose at the liquid-air interface (Fig 18). This pellicle was then removed (Fig 19), and the solution was re-incubated with an additional 200 mL of GYC media allowing for the bacterial culture to produce additional cellulose pellicles.

The pellicle was then placed into falcon tubes with holes melted into the lid. The falcon tubes were freeze dried for 48 hr to reduce the viability of any microbial organism's present. The pellicle was then removed and suspended in a Durnan flask with 200 mL of 1% NaOH for 1 hr at room temperature. The flask was then submerged in boiling water for 30 min and centrifuged



Figure 19: Biocellulose pellicle.

at 6000 RPM for 20 min. The pellicle within the flask was then washed with RO H₂O and centrifuged for another 20 min. The pellicle was then suspended in Cross-Beaver reagent (200 mL 1 M HCl with 100 g ZnCl₂) for 24 hr to dissolve the cellulose pellicle.

Four volumes of 95% ethanol were then added to the solution and placed on a shaker at room temperature in order to aid the precipitation of the nanocellulose material. The solid nanocellulose was then centrifuged at 6000 RPM for 20 min, dissolved in RO H₂O and placed into dialysis tubing. The tubing was submerged in RO H₂O and stirred gently to remove any small degraded particles while retaining the nanocellulose.

Finally, the contents of the dialysis tubing were removed and centrifuged at 2000 RPM for 10 min then freeze dried for 24 hr to produce the purified nanocellulose.

This nanocellulose was then TEMPO oxidised to produce processed bionanocellulose and isolated using the same technique provided in 3.1.3.

3.1.3 TEMPO

TEMPO oxidation of the treated fibres was used to prepare the cellulose microfibrils for hydrogel formation.

1 g of pre-TEMPO cellulose microfibrils was stirred in a beaker with 200 mL of RO H₂O for 1 hr. 0.1 g of NaBr with 0.016 g of TEMPO as a catalyst was then added to the beaker; the solution was stirred on high for a further 30 min.

26.5 mL sodium hypochlorite solution was then added and the solution continued to be stirred until the reaction had completed. This reaction required the solution to be maintained at pH 10 with dilute sodium hydroxide and dilute hydrochloric acid used to alter the pH. When the pH change was less than 0.2 over the course of 1 hr, the reaction was completed (\approx 12 hr). After the reaction was completed, it was quenched with 1 mL of ethanol and the pH was set to 7.

The solution was then filtered and the solid product was washed four times with RO H₂O. The fibres produced were colourless with a gel like texture. This material was then placed into the freeze drier overnight, producing a soft white solid (Fig 20).⁵⁴



Figure 20: Purified nanocellulose.

3.2 Hydrogel preparation

3.2.1 Sodium alginate mixed hydrogels

For this study 0.27 g sodium alginate was mixed with 0.03 g TEMPO oxidised nanocellulose at a ratio of 1:9 with 30 mL of 10 mg/mL butorphanol to form a 1 m/V% hydrogel. Negative controls of pure sodium alginate and TEMPO oxidised nanocellulose were also produced. The solutions were then homogenised.

3.2.2 Chitosan mixed hydrogels

Chitosan hydrogels were prepared following the same method detailed in 3.2.1 with high quality NaOH treated chitin replacing the sodium alginate.

3.2.3 Dry NC-SA hydrogel swelling and release patterns

To determine the swelling rates for dry hydrogels, combinations of TEMPO oxidised nanocellulose and sodium alginate at ratios of 1:0, 1:9, 1:1, 9:1 and 0:1 were prepared in 20 mL of RO H₂O. The nanocellulose was suspended in 10 mL RO H₂O and sonicated for 1 hr, the sodium alginate was dissolved in 10 mL RO H₂O and stirred for 2 hr.

The nanocellulose was then added to the sodium alginate, stirred for an additional hour then homogenised for 5 min to produce a viscous solution. The solution were then poured into a petri dish, placed in a 60°C oven for 24 hr and then freeze dried for 24 hr to produce a dried hydrogel.

This was repeated for all of the NC:SA ratios.

The hydrogel was then suspended in 20 mL of a 5% solution of CaCl₂ for 24 hr according to previous studies conducted with sodium alginate hydrogels⁵⁵, oven dried at 60°C for 24 hr and freeze dried for 24 hr to produce the final dried hydrogel.

The dried hydrogel masses were measured and then placed into a beaker of 200 mL RO H₂O to re-hydrate and swell the hydrogels, in order to determine the water absorption rate. After the hydrogels had been incubated for 30 min, the hydrogels were removed and placed on filter paper briefly to remove peripheral water then weighed to determine the H₂O absorption rate according to eq (1).

$$WA = \frac{Mw - Md}{Md} * 100 \quad (1)$$

WA is the water absorption rate, Mw and Md are the wet and dry masses respectively.

The swollen hydrogels were then centrifuged for 3 min at 3500 RPM to determine the water retention rate of the hydrogels according to eq (2)

$$WR = \frac{Mh - Md}{Md} * 100 \quad (2)$$

WR is the water retention rate, Mh and Md are the masses after centrifugation and initial dry weights respectively.

3.2.4 NC-SA hydrogel gel preparation

3.2.4.1 Preparation of hydrogel for animal testing

Nanocellulose and sodium alginate hydrogels were prepared for animal testing from the nanocellulose prepared in 3.1.3 and sodium alginate. 0.03 g of the nanocellulose was placed into 15 mL of RO H₂O and sonicated for 1 hr to begin breaking down and dissipating the nanocellulose clumps. 0.27 g of sodium alginate was then stirred in 15 mL of RO H₂O for 2 hr until it had completely dissolved.

The solutions were then combined and stirred for a further 2 hrs, then the solution was homogenised for 5 min to form a uniform clear viscous solution. This solution was then poured into a sterile petri dish and freeze dried for 24 hr.

The freeze dried gel was then re-suspended in 30 mL of 1% CaCl₂ solution to facilitate ionic crosslinking and increase the stability of the gel. This solution was stirred for 6 hrs and then homogenised for 5 min to produce a more viscous yet still clear solution as seen in the previous step. The solution was poured into a sterile petri dish and freeze dried for a further 24 hr.

The dried gel was then re-suspended in 30 mL of 10mg/mL butorphanol, stirred for 6 hrs, homogenised for 5 min and then stirred for 12 h to ensure the drug had loaded onto and into the hydrogel. This 30 mL of hydrogel was then used for the animal testing.

All stirring steps occurred at 4°C in a sterile environment to reduce the risk of microbial contamination and degradation of the hydrogel.

3.2.4.2 Preparation NC-SA hydrogels for drug release in RO H₂O

To prepare the NC-SA hydrogels, 0.03 g of nanocellulose, prepared using the method detailed in 3.1.3 was suspended in 15 mL of RO H₂O and sonicated for 1 hr. 0.27 g of sodium alginate was suspended in 15 mL RO H₂O and stirred at high speed for 2 hr. The nanocellulose and sodium alginate solutions were then combined, stirred on high for 1 hr and then homogenised for 5 min. The solution was then poured into a sterile petri dish and freeze dried for 24 hr.

The freeze dried solution was then re-suspended in 30 mL of a CaCl₂ solution. This solution was stirred on high for 6 hrs and then homogenised for 5 min. The solution was poured into a sterile petri dish and freeze dried for 24 hr.

The dried gel was then re-suspended in 30 mL 10 mg/mL butorphanol, stirred for 6 hrs, homogenised for 5 min and then stirred for 12 hr. The concentration of CaCl₂ solutions used were 0.5 molL⁻¹, 1 molL⁻¹, 1.5 molL⁻¹.

3.2.4.3 Preparation of chitosan-SA hydrogels for drug release in RO H₂O

This preparation was done identically to 3.2.4.2 with the following alterations. Sodium alginate was replaced with chitosan and the CaCl₂ concentration was set at 1 mg/mL.

3.2.5 Hydrogel drug release in RO H₂O

The prepared hydrogels were taken from the freeze drier and placed into 200 mL beakers. 100 mL of room temperature RO H₂O was gently poured into the beaker with care taken to prevent disruption of the gel film.

A small stirrer bar was placed into the beaker and stirring commenced at a low speed (setting 1)

The gel film would float to the top of the vessel for 2-3 min before absorbing enough liquid to allow it to settle onto the bottom as a distinct layer roughly 2-3 cm thick.

At 15 min a 1 mL sample was taken from the water layer (1 cm below surface air interface) and 1 mL of fresh RO H₂O was added to maintain the volume of the vessel at 100 mL.

This was repeated at time intervals of 30 min, 1, 2, 4, 6, 12, 24 hrs.

These samples were then centrifuged at 13,000 RPM for 2 min and analysed using the using HPLC following the methods detailed in 3.4.3 and 3.4.4.

3.3 Avian testing

3.3.1 Animal trials

The animal trials were conducted by Dr Preet Singh, School of Veterinary Sciences, Massey University. The protocol for this experiment was approved by the Massey University ethics committee.

The *pilot* trial used six broiler chickens with an average live weight of 2 kg.

The *primary* study involved 16 broiler chickens with an average live weight of 3.5-4.5 kg. This study had six chickens injected with the nanocellulose-alginate hydrogel (treatment group) described in 3.2.4 and six chickens injected with commercial formulation of butorphanol (control group).

Four of the chickens were kept for blank plasma collection and to be used as replacements if any of the other chickens died or could not have catheters inserted due to damaged veins or uncooperative nature.

Each chicken was catheterised with a 22 G catheter into the medial metatarsal vein after gentle restraining of the bird. The catheters were firmly fixed by wrapping the catheterised leg with cohesive bandage. The patency of the catheters were maintained by flushing with 0.5 mL 10% heparin- solution.

The chickens were kept under standard conditions and were fed *ab lib* with commercially available chicken feed and a 24 hr supply of fresh drinking water was made available. The catheters had heparin inserted to prevent coagulation and clotting of blood within the catheter.

3.3.2 Drug administration

The control group chicken received Butorphanol tartrate 10mg/mL (Butorphic Injection; Llyod Laboratories) at 6 mg/kg dose, subcutaneously using a 22G needle at midline caudo-dorsal region of the neck. The treatment group chickens received nanocellulose alginate formulation of butorphanol subcutaneously at a similar dose (Table 2) and site of injection as the control group.

Table 2: Primary study. Chicken number with associated weight and volume of 10 mg/ml hydrogel / butorphanol injected. 6 mg/mL dosage. Chicken G were injected with the NC:SA hydrogel formulation. Chicken NG were injected with commercial 10 mg/mL butorphanol.

Chicken G #	Weight (Kg)	Injection (mL)	Chicken NG #	Weight (Kg)	Injection (mL)
1	3.3	2.0	1	4.1	2.5
2	3.5	2.1	2	4.2	2.5
3	3.7	2.2	3	4.0	2.4
4	3.8	2.3	4	4.3	2.6
5	3.9	2.3	5	4.1	2.5
6	3.6	2.2	6	3.9	2.3

3.3.3 Serum collection

The broiler chickens from the *pilot* study had 1 mL and the chickens from the *primary* study had 2 mL blood samples serially collected.

The samples were collected at 0, 15, 30, 60 minutes and 4, 8, 16 and 24 hrs after injections of commercial butorphanol and 0, 15, 60 minutes and 2, 4, 8, 16, 24, 32, 48, 72 and 96 hr after injections of the hydrogels loaded with butorphanol (Appendix i,ii).

After collection, the blood samples were placed into an ice bath to cool then centrifuged for 10 min at 2000 RPM to separate unwanted materials from the plasma containing the butorphanol. The plasma samples were then isolated and placed into a -70°C freezer for storage.

3.4 Sample preparation

3.4.1 HPLC analysis preparation

The chicken plasma samples were stored at -70°C, the samples were defrosted at room temperature in water to speed up the defrosting process. 300 µL of the chicken plasma sample was then removed for testing and the remaining sample was immediately returned to the -70°C freezer for further analysis if required. Some samples were frozen then defrosted multiple times and there was no adverse effect upon the HPLC results observed when compared to the initially defrosted samples results.

300 µL of chicken plasma was diluted with 300 µL of RO H₂O and vortexed for two minutes to ensure even distribution of the plasma within the solution. 300 µL of 2 M HCl was then added to the sample and vortexed to maximise the exposure of the blood plasma to the acid. The solution was then centrifuged at 13,000 RPM for ten minutes to sediment the unwanted particles, separating them from the desired supernatant for SPE loading.

3.4.2 Solid phase extraction

Phenomenex Strata-X 30 mg/1 mL Polymetric Reversed Phase SPE cartridges were preconditioned with 1 mL of 100% methanol and then equilibrated 1 mL of RO H₂O while under vacuum filtration. The supernatant from the samples was then loaded into the pre-conditioned SPE cartridge and run under vacuum filtration until dry.

After the serum was loaded, the SPE tubes were washed with 1 mL of RO H₂O, run until dry and then left under vacuum for a further two minutes. An additional wash of 1 mL 40% methanol was then added and left under vacuum suction for a further two min. A 1 mL sample of 100% methanol was then added to elute the butorphanol from the SPE cartridge where it was collected into 5 mL test tubes.

These tubes were then dried under reduced pressure at 20°C with centrifugation at 13,000 RPM for 10 min. The sample was then reconstituted in 200 µL of the mobile phase (2:8 acetonitrile: 0.1 M phosphate buffer pH 4), placed into HPLC vials containing inserts to reduce the risk of needle tracking errors and placed into the HPLC loading rack which was kept at 4°C.

3.4.3 HPLC preparation protocol

The two feed lines were placed into Duran bottles containing 0.1 M pH 4 phosphate buffer and 100% acetonitrile respectively with aluminium foil sealing the lid, then the valves were opened bypassing the HPLC column and the system was purged to remove any air bubbles present in the lines which could cause problems with the HPLC. The acetonitrile had already been placed in a sonicator on degassing setting for 10 minutes to remove any bubbles present.

After the system had purged the valves were closed and the 80% gradient of 0.1 M pH 4 phosphate buffer to 100% acetonitrile was run at a flow rate of 0.2 ml/min for 2 min, it was then increased by 0.2 ml/min every 2 min until it reached the desired flow rate of 1ml/min. It was then run at this rate for 30 min before the HPLC run was begun to ensure any contaminant in the column that had not been removed by the cleaning protocol would have been removed and the HPLC column would have a uniform surface.

3.4.4 HPLC run protocol

Sample injection volumes of 50 µL were done in duplicate with the samples cooled to 4°C and the column set at 40°C. There was a run time of 15 min under isocratic conditions with a binary gradient of 80% phosphate buffer with 20% acetonitrile and a flow rate of 1 mL/min to separate the butorphanol peak from other peaks present in the solution.

The UV absorption was measured from 200-280 nm, the peaks that were observed when the absorption was at 202 nm were used to calculate the butorphanol concentration.

3.4.5 HPLC cleaning protocol

The system was cleaned after every sample set had been run to avoid contamination of sequential samples and pressure increases due to clogging of the guard column and HPLC column by precipitation of the salts in the buffer

This cleaning involved placing the feed lines into a Duran bottle containing RO H₂O and purging the system with the same method detailed in 3.4.3.

After purging the valves were closed and the HPLC column was removed and placed aside. Both feedlines then had their flow rates set to 2.5 mL/min and run for 5 min. The pumps were then tuned off, the HPLC column was reattached, the flow rates were set to 0.2 mL/min and the pumps turned on again for 30 min.

The pumps were then turned off and the feedlines were placed into Duran flasks containing a solution of 50:50 acetonitrile:RO H₂O. The system was purged following the same procedure then run at a 0.2 mL/min flow rate for each feedline for 30 min.

3.5 HPLC Validity

3.5.1 Butorphanol recovery

To determine the recovery rate of butorphanol from SPE cartridges, blank serum samples were spiked with 300 µL of each known concentration used in the butorphanol standard curve. The butorphanol solutions replace the RO H₂O step of solid phase extraction. The HPLC run protocol remains unchanged.

The spiked plasma samples were run in triplicate with the peak area, height and retention time compared to the results from the butorphanol standard curve.

This was done to determine the recovery rate of butorphanol after SPE.

3.5.2 HPLC specificity

Blank plasma from 16 broiler chickens was extracted from blood samples and analysed using HPLC after SPE to determine the specificity of the method.

3.5.3 HPLC analysis

Standard curves were constructed using the butorphanol standard curve at the beginning the alternating plasma samples and butorphanol standard curve. These samples were run in duplicate using the HPLC run protocol.

3.5.4 Chromatograph analysis

The chromatograph readings for the butorphanol standard curve and plasma samples were analysed for peak area, height and retention time. The concentration of butorphanol contained within the plasma samples was then calculated by comparing the peak results to a calibration curve produced by the butorphanol standard curve. This was all calculated using LC solution software with manual integration used for peaks with a height below 200 or areas below 500.

3.5.5 New Column

A standard curve of butorphanol standards in mobile phase from 1 µg/mL, 500 ng/mL, 250 ng/mL, 125 ng/mL, 62.5 ng/mL, 31.2 ng/mL and 15.6 ng/mL was run on the new column in triplicate with the same protocol as 3.4.4. The chromatograph was then analysed to determine the maximum and minimum concentration that could be accurately determined.

3.5.6 HPLC Linearity

This butorphanol standard curve was run in triplicate using the same HPLC technique used for the HPLC run protocol. This data obtained was then analysed and subjected to linear regression in LC solution software to determine if there was any variation in intraday samples.

3.6 Data analysis

Variance is calculated for the butorphanol standard curve, the HPLC chromatograph area and height data and averages.

The formula is:

$$\text{Variance} = \text{VAR. } P(x1: xn) / \text{AVERAGE}(x1: xn) \quad (3)$$

x1 = initial value, xn = final value

This is then used to calculate the percentage variance:

$$\%V = 100 - ((A/(A + V)) * 100) \quad (4)$$

A = Average area/height, V = Area/height variance

The concentration is then calculated from the butorphanol standard curve results which produce a linear line of best fit. The formulae of the line are then used to determine the concentration of the samples based upon area and height.

The RO H₂O hydrogel release study required an additional calculation to negate the effect of removing 1 mL samples and replacing with 1 mL fresh RO H₂O.

$$\text{Adjusted conc} = \text{conc} * \left(\frac{100}{(100 + (n - 1))} \right) \quad (5)$$

n = sample number

The results were graphed with the concentration calculated using the average areas vs time and the concentration calculated using the average heights vs time.

The original 300 μL of chicken serum sample were reduced to a 200 μL final volume. The calculated concentration of the sample was adjusted to take into account this deviation. The formulae used was

$$\text{Adjusted conc } \left(\frac{\text{ng}}{\text{mL}}\right) = (\text{Original conc } \left(\frac{\text{ng}}{\text{mL}}\right) * 0.2) / 0.3 \quad (6)$$

3.6.1 Statistical analysis

The pharmacokinetic parameters from three different groups calculated by the methods described above were compared by one-way ANOVA non-parametric using Prism 6 for Macintosh (GraphPad Software, Inc, CA, USA). The multiple comparisons were made by Kruskal-Wallis test. Significance was set at $p < 0.05$.

3.6.2 Pharmacokinetic analysis

Pharmacokinetic parameters were determined using noncompartmental analysis. PKSolver 'add-on' for Excel 2010⁵⁶ was used to calculate pharmacokinetic parameters using individual plasma concentration data.

4. Results and discussion

4.1 Pre-TEMPO chemical preparation

In addition to the desired cellulose, the raw stock hemp fibres contained numerous compounds which needed to be removed before the cellulose could be extracted and processed. The initial steps removed the fatty lipids from the hemp fibre surface using an acetone:water solution followed by separation of the pectin, lignin and other chemical components such as tannins and hemi-cellulose from the desired cellulose. This was done according to the modified Wise method detailed in 3.1.1.

The multiple washes with RO H₂O after acetone:water treatment ensured the removal of any remaining water soluble impurities. The sample was then dried to remove the remaining water and acetone. This was done to prevent it interfering with the NaClO₂ solution. Any water present would have changed the weight of the hemp fibres which would have altered the hemp weight to volume NaClO₂ ratio used, potentially changing the degree of ligand removal.

The modified Wise method was performed at 70°C to increase the rate of reaction between NaClO₂ and any ligand compounds while also causing heat degradation of the hemp structure. This reduced the structural integrity of the hemp fibres and increased the permeability, allowing the NaClO₂ to penetrate further and remove a higher percentage of the ligands present.

The NaClO₂ was added to remove any lipids present in the solution. It was done in multiple washes to ensure that there was fresh NaClO₂ to act upon any remaining lipids after the heat had begun to degrade the fibres over time. The longer run times than the original Wise method allowed the fibres to form a much finer white solid which had a larger exposed surface area for TEMPO oxidation. This also increased the amount of fibres that formed nano-fibrils instead of micro-fibrils which were preferable for hydrogel formation.

The final steps involving the commercial blender were to maximise the mechanical breakdown of the fibres before TEMPO oxidation. This increased the surface area of hemp fibre available for the TEMPO reaction to affect and produced higher quality cellulose microfibrils. The material loss from the transfer between the blender and beakers was considered to be an acceptable loss.

4.2 Bionanocellulose preparation

The initial cultures of *G. xylinus* were taken from frozen glucose stocks, they were known to still be viable and were believed to be capable of producing the levels of cellulose desired. These cultures were then plated out onto GYC agar that was capable of growing the microbe to the desired levels at the ideal growth temperature of 30°C without excessive treatment being required. This ensured that there were enough colonies available for incubation in the GYC media without contaminants.

The cultures required access to oxygen and the prevention of airborne microbes from contaminating the sample. To solve these problems, a cotton wool plug was placed into the neck of the flasks and was considered to be a suitable solution as a microbe filter.

The three stages of upscaling for the liquid media chosen were a 10 mL test tube, a 250 mL Duran flask and 2 L Erlenmeyer flasks.

The test tube had a low surface area to volume ratio so was not suitable for large scale production. The pellicle formed on the liquid air interface. This decreased the oxygen content of the solution which is required by the aerobic *G. xylinus*. However, it did allow for the growth of the microbe to be easily identified as well as determining if there was any contamination by other microorganisms without wasting large volumes of GYC media.

The 250 mL Duran flask had a greater surface area to volume ratio but lacked the required surface area and nutrient levels for production of larger pellicles. It was however, a very useful step in the scale up process. It provided a final check to ensure that there was no contamination present before the final upscaling step which had the largest GYC media requirement.

The 2 L Erlenmeyer flask proved to be the most suitable for large scale production. It produced a thick pellicle which could be harvested. The culture could then be re-incubated to produce multiple pellicles provided the solution was not contaminated by other microbes and that there were suitable levels of oxygen and nutrients present in the solution. This however proved to have diminishing returns with smaller pellicle sizes and repeated harvesting dramatically increased the risk of contamination. Even when conducted under aseptic conditions, the non-specific nature of the media allowed fungal colonies to grow rapidly if exposed to the solution.

Maintaining a sterile environment when working on the cultures proved difficult due to the large volumes and multiple transfers leading to fungal contamination of one of the cultures. This only became prevalent in one culture when the 2 L flask was re-incubated after removal of the cellulose pellicle. In one preparation, the fungal contamination resulted in a disrupted and mechanically weaker cellulose pellicle thought to be due to either competition for nutrients or an antibiotic effect caused by the fungal species causing bacterial cell death. This pellicle was degraded during isolation so was therefore unusable.

The initial bionanocellulose pellicles produced had an average freeze-dried weight of 0.8 g after 3 weeks incubation. The processed weight however was only 0.12 g and with the normal 54% yield loss due to TEMPO oxidation demonstrated by the hemp nanocellulose it was decided not to continue with the TEMPO oxidation.

The experiment was re-attempted with a 6-week incubation time for the 2 L Erlenmeyer flask step. This produced a much thicker pellicle with a stronger binding. The freeze-dried weight was 2.1 g but after further processing the final weight came to 0.74 g. This was then treated with TEMPO oxidation in the same manner as the hemp fibres in 3.1.3. The final weight came to 0.25 g but this was deemed to be insufficient for production of hydrogels.

Subsequent growth attempts lead to similar results believed to be a result of the colony strain not being suitable for large scale bionanocellulose extraction. This preparation was therefore discarded in favour of the top-down nanocellulose extraction from hemp fibres which had a far lower time requirement. Larger quantities of the initial raw material were available. This methodology was capable of producing usable amounts of nanocellulose for hydrogel production.

4.3 TEMPO oxidation

The initial 1 hr stirring step ensured that the cellulose microfibrils were dispersed in the solution and any clumps were disrupted. This maximised the surface area exposed to the solution. This was done to maximise the reaction rate and permeation. This increased the proportion of nanocellulose produced from the microcellulose for hydrogel formation.

Figure 21: TEMPO oxidation of cellulose.⁸

TEMPO is a stable nitroxyl radical with many applications in organic chemical and biochemical processes⁵⁷. For one of the primary chemical processes, TEMPO is used as a catalyst in the presence of NaBr to cause the conversion of pseudo amorphous cellulose into the polyglucuronic acid sodium salt with NaOCl as the catalytic reagent (Fig 21). Maintenance of pH 10 is required to reduce the degradation of the polymer chains and the accumulation of unwanted side products which would reduce the amount of usable nanocellulose for hydrogel formation.

After freeze drying, the processed samples gave an average percentage yield of 46% (Table 3). The decreased percentage yield is believed to have been a result of the TEMPO oxidation breaking down some of the cellulose polymer chains to produce short chain molecules which could not be recovered. There were also transfer losses when the processed nanocellulose was extracted via vacuum filtration as the colourless gel was difficult to observe and formed films upon the sides of the filter as well as the filter itself preventing recovery without contamination with fibres from the filter.

Modification of the cellulose chains allowed formation of multiple C₆ carboxylate groups which assisted in the formation of strong hydrogels from mixed preparations. This occurs because of the interactions between the post TEMPO nanocellulose and other compounds with carboxyl groups when crosslinked with calcium ions forming ionic bonds (Fig 22).

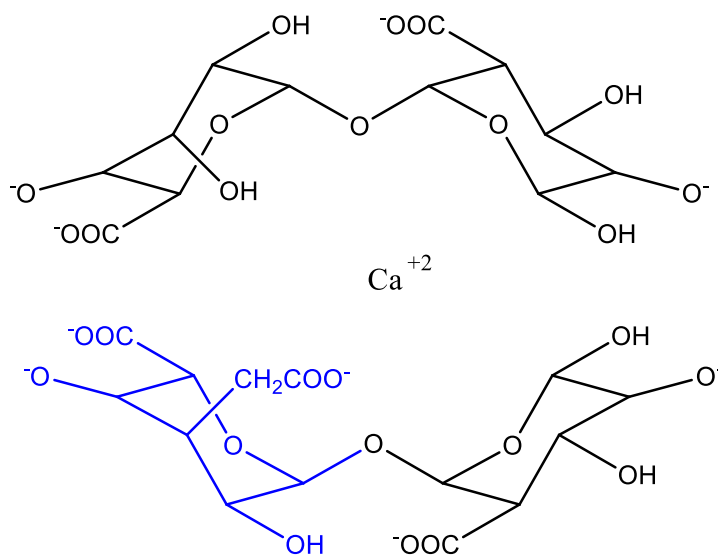


Figure 22: TEMPO oxidised cellulose (Blue) and sodium alginate (Black) chains crosslinked with CaCl₂.

Table 3: Yield from multiple runs of TEMPO oxidation on cellulose fibres.

Run	Pre-TEMPO cellulose mass (g)	Post-TEMPO cellulose mass (g)	Difference (g)	% Yield
1	1.01	0.48	0.53	47.5
2	1.03	0.50	0.53	48.5
3	0.98	0.44	0.54	44.9
4	1.00	0.45	0.55	45.0
5	1.04	0.49	0.55	47.1
6	1.06	0.49	0.57	46.2
7	0.99	0.44	0.55	44.4
Average	1.02	0.47	0.55	46.3

4.4 Nanocellulose optimisation

Processing of hemp fibres to extract cellulose fibrils with a nanometer dimension uses many traditional techniques such as acetone treatment and TEMPO oxidation. Due to the coarse nature of the fibres compared to the cotton fibres traditionally used, alterations were required to the techniques to optimise the yield.

The initial removal of lipids from the hemp fibres using an acetone:water mixture had the treatment time increased to 48 hr from 24 hr. This made the fibres become soft and white with a cotton like texture instead of rough brown woody fragments.

The NaClO₂ shock treatment of the treated hemp fibres was extended from four shocks of two hour duration each, to five shocks of three hour duration each. This produced softer fibres which had begun to break down. They could then be mechanically degraded further using a blender.

The degraded hemp fibres were more easily oxidised to a greater degree using TEMPO than fibres produced using the traditional techniques.

The TEMPO oxidation technique from 3.1.1 was unchanged from the literature except for a two hour extension of the incubation period until the pH change of the solution had slowed to less than approximately 0.5 pH/hr. Then the solution was left overnight to produce a final average pH reading of 9.4 before it was quenched with ethanol and set to pH 7.

4.5 Hydrogel preparation

There have been many polysaccharides which have been used to form hydrogels. The two most commonly used are sodium alginate extracted from the cell walls of algae and chitosan produced from chitin which is extracted from the shells of shellfish. Therefore, two polysaccharides were considered for a combination hydrogel preparation with nanocellulose. Due to the limited timeframe available for the project, sodium alginate was chosen to be combined with nanocellulose fibrils. This was decided as the sodium alginate was readily available in high quality and could be crosslinked with nanocellulose.

Chitosan was briefly examined as a potential hydrogel material as it had similar characteristics to sodium alginate. It was also available in acceptable quantities and could be crosslinked with nanocellulose using CaCl₂.

4.5.1 Dry NC-SA hydrogel swelling patterns

Dry hydrogel water absorption and water retention rates were outside of the expected range. Previous sodium alginate studies had shown water absorption and retention rates at 10-fold and 5-fold higher levels respectively. This was later decided to be a result of the higher strength of the hydrogel matrix.

The water absorption rates obtained showed consistent rates across the triplicates studied but the maximum absorption rate for the 1:9 NC:SA gel had an average rate of 91% increase compared to the literature study with 1040%. The maximum water retention rate was 85% compared with the 569% from the literature.⁵⁵

The other hydrogel compositions had lower absorption and retention rates than the 1:9 NC:SA ratio hydrogels. It was therefore decided that while the WA and WR rates were far lower than expected this provided confirmation that the 1:9 NC:SA ratio was the most efficient available.

The lower rates could be explained by the nature of the nanocellulose. The nanocellulose extracted from hemp possessed a far higher mechanical strength than the nanocellulose extracted from cotton used in the literature. This resulted in the stronger hydrogel lattice. The stronger hydrogel lattice would have restricted the swelling potential and this would also have affected the water release rate by restricting the contraction of the hydrogel.

The cellulose content of cotton was far higher with an average of 94% while hemp pulp has an average cellulose content of 40-45%.⁹ This meant that the cotton fibres required less intense treatment which may have resulted in the hydrogels produced to have a lower density, allowing for more water to be taken up into the matrix and retained.

4.5.2 RO H₂O NC-SA hydrogel release

The concentration of CaCl₂ was altered to determine the optimal amount of crosslinking required to produce suitable hydrogels. The hydrogel needed to be capable of taking up and retaining the drug while maintaining their matrix structure to allow for a prolonged release rate. The hydrogel was also required to be viscous enough to allow subcutaneous injection with a 22G needle.

Calcium chloride was chosen as the crosslinking reagent. It produced Ca^{2+} ions capable of forming an ionic bridging bond between two polymer chains and had been commonly used in other studies. Other bridging compounds such as magnesium chloride were briefly considered but were not investigated due to time restrictions and the efficiency of CaCl_2 .

The three concentrations of CaCl_2 were chosen to provide a wide concentration range. This would produce a hydrogel that would be crosslinked together to form a more viscous gel while still being injectable. The lowest concentration CaCl_2 produced a very fluid gel that had released 90% of the drug into solution within the first hour. This was decided to be inadequate as the hydrogel would ideally decrease the drug release rate so it would continue to release an effective dose for multiple days.

After 6 hrs there was depreciation in the drug level detected within the sample from the 0.5% CaCl_2 hydrogel. This is potentially caused by the hydrogel degrading and the individual polymer chains binding to the butorphanol in solution, isolating the drug to the lower levels of the vessel. The samples were taken from the upper layer and therefore if the hydrogel components bound the butorphanol, some of the butorphanol would sink to the bottom of the beaker would be unavailable, decreasing the overall concentration of the solution.

The samples were taken from the top of the vessel to prevent uptake of any hydrogel that could alter the samples concentration after processing. The samples were centrifuged to remove any solid components that may produce blockages within the HPLC or corrupt the results.

This may cause any hydrogel components that were taken up in the sample to release the encapsulated butorphanol. This would cause a spike in the butorphanol concentration of the sample (Graph 3), artificially increasing the calculated release rate (Table 5).

This is likely why there was a large spike in butorphanol concentration at the 30 min sample for the 0.5% CaCl_2 gel (Graph 3). The gel had not settled completely at the base of the vessel and the structural rigidity of the gel was the weakest due to the lowest amount of crosslinking present. This may have caused some hydrogel to be present in the sample extracted resulting in the observed concentration spike after the sample had been processed.

The 1% CaCl₂ gel exhibited the best release rate of the butorphanol, it had the slowest release rate observed and the concentration of butorphanol in the solution remained relatively constant after 6 hrs. This is likely due to the structural rigidity of the gel allowing uptake of the butorphanol while also being capable of tolerating the agitation caused by the stirrer bar without disrupting the hydrogel matrix.

The 1.5% CaCl₂ gel showed the most rapid drug release rate. The majority of the drug had been released within the first hour. This was not desirable as the aim was to produce a long-term release gel. The rapid release rate was believed to be a result of the crosslinked hydrogel preventing uptake of the butorphanol into the gel. Instead the drug was mostly confined to the peripheries of the gel. When the gel was submerged in RO H₂O the bonds connecting the butorphanol to the hydrogel peripheries were disrupted resulting in a large amount of free butorphanol in the solution.

The 1% CaCl₂ gel was considered to be the ideal balance between a robust hydrogel capable of surviving longer periods in solution without physical changes. It also formed a hydrogel with a density capable of taking up butorphanol into the matrix, lowering the drug release rate.

The 1% CaCl₂ was chosen as the most appropriate gel for the animal trials and therefore studies proceeded with a 3% m/V 1:9 NC-SA 1% CaCl₂ gel.

4.5.2 Wet NC-SA hydrogel preparation

4.5.2.1 Pilot study

The hydrogels were initially prepared with a 1 m/V% 1:9 NC:SA composition. This was due to the processed nanocellulose being scarcer, more expensive than the sodium alginate and based on the results obtained in 4.5.1. In order to produce a larger number of replicable gels, the lower NC:SA ratio was used with further release studies planned with the higher NC:SA ratios to determine an optimal ratio to balance efficiency and cost.

The other consideration was the viscosity of the hydrogel, the administration into the chicken involved a subcutaneous injection. This made highly viscous gels with large scale crosslinking impractical. The 1% m/V 1:9 NC:SA gel with 1 mL of 1% CaCl₂ had at that stage of the project, the highest viscosity while still being capable of being delivered via injection to the broiler chickens.

This was later improved with modifications to the processing steps for nanocellulose producing hydrogels that had limited clumping at higher concentration hydrogels.

The butorphanol concentration in the gels was 10 mg/mL. This was chosen as it was within the tolerance range of the chickens if the gel degraded and released the drug faster than expected. The butorphanol level was also high enough that if the release rate was slower than expected, the levels present in the serum would remain detectable.

The results from the pilot studies showed that the release rate of the hydrogel was higher than desired. However, due to limited amounts of available serum and complications with the HPLC, the results were too variable for detailed analysis and were therefore discarded.

4.5.2.2 Primary study preparation

After the *pilot* study, it was discovered that with some changes in the processing steps to form nanocellulose a suitable hydrogel could be produced. The problem with the low concentration of the hydrogel was removed by improved processing of the nanocellulose fibrils and alterations to the hydrogel formation technique, disrupting any nanocellulose clumps present in the hydrogel.

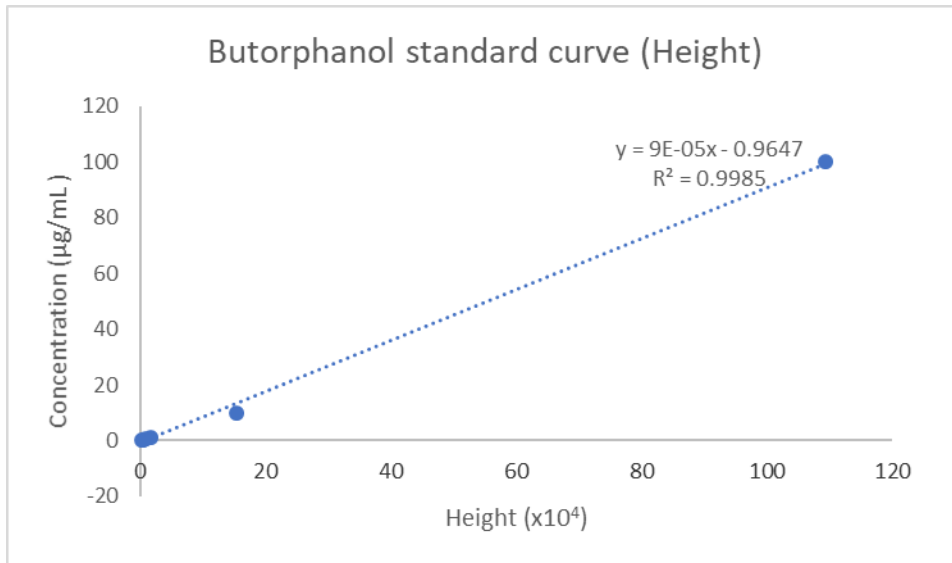
With the higher concentration of hydrogel now available for consideration, more modifications could be investigated. After further analysis and experimentation, it was found that it was possible to form a 3 m/V% 1:9 NC:SA gel with 1 mL of 1% CaCl₂. The hydrogel was evenly dispersed within the solution, had a viscosity that was low enough to be easily injected and displayed the best release rate in the RO H₂O study.

The hydrogel was then tested in-vitro in chickens as discussed in 3.3 and analysed by the techniques detailed in 3.4 and 3.5.

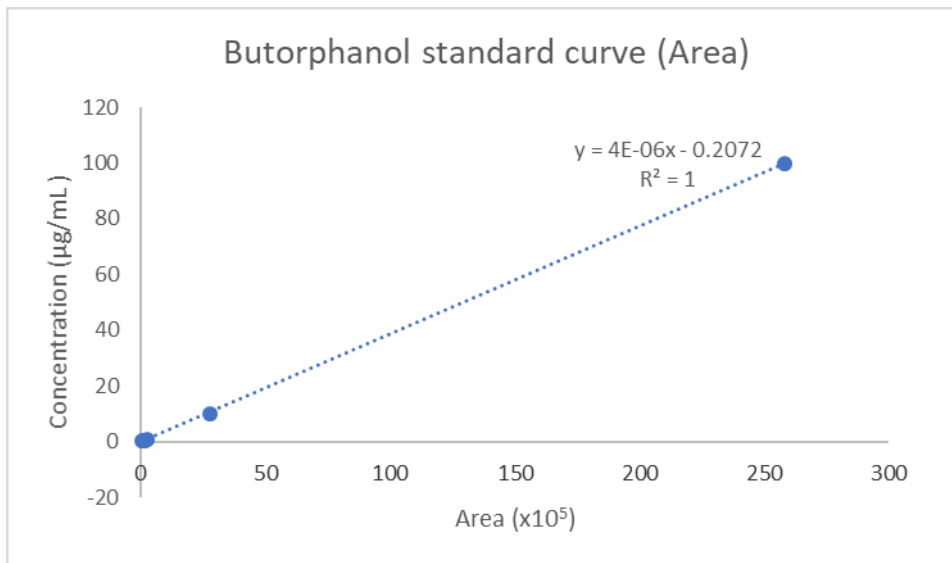
4.5.3 Hydrogel release in RO H₂O

The hydrogel release rates were measured against the butorphanol standard curve to provide context to the area and height measurements from the sample peaks. The peak area vs concentration graph had the linear trendline with the R² value closest to 1. The equation of the line was then used to calculate the concentration of the adjusted samples (Graph 1).

Graph 1: Butorphanol level vs HPLC peak area



Graph 2: Butorphanol level vs HPLC peak height



This reduced the risk of misinterpreting the HPLC results for the samples and clearly showed that the inter-day accuracy of the samples was high. The area variation was below 2% for the area samples with the exception of the 250 ng sample, this had an outlier increasing the variation to $\approx 4\%$ (Table 4). The peak height inter-day variation was lower ($> 0.25\%$) but had a linear line of best fit that had a lower R^2 value so it was not used (Graph 2).

Table 4: Butorphanol standard solutions with variance and percentage variance. The low variance values show that the inter-day samples are consistent.

Butorphanol	Average Area	Average Height	Area Variation	% Area variation	Height Variation	% Height variation
100ug	$2.58 * 10^7$	$1.094 * 10^6$	$2.22 * 10^3$	0.203	186	0.0170
10ug	$2.77 * 10^6$	$1.54 * 10^5$	285	0.184	18.6	0.0121
1ug	$2.77 * 10^5$	$1.65 * 10^4$	312	1.85	1.07	0.00650
500ng	$1.53 * 10^5$	$8.79 * 10^3$	173	1.93	0.749	0.00852
250ng	$8.82 * 10^4$	$4.70 * 10^3$	192	3.93	11.3	0.240
125ng	$5.06 * 10^4$	$2.50 * 10^3$	29.3	1.16	1.39	0.0555

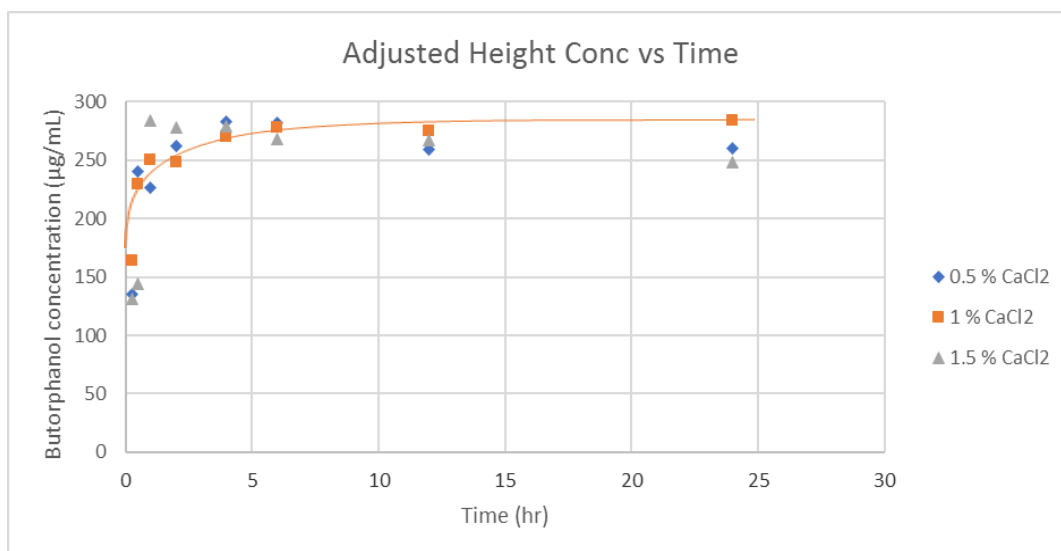
The butorphanol levels of the samples were calculated using the STD butorphanol standard curve (Table 4). The concentrations taken from the STD standard curve had to be adjusted to take into account the removal of 1 mL of sample and its subsequent replacement with RO H₂O which diluted the total solution.

The samples did contain a higher drug concentration than the highest STD butorphanol standard curve concentration but the linear nature of the previous results and previous experimentation with higher concentrations made this assumption reliable.³⁴

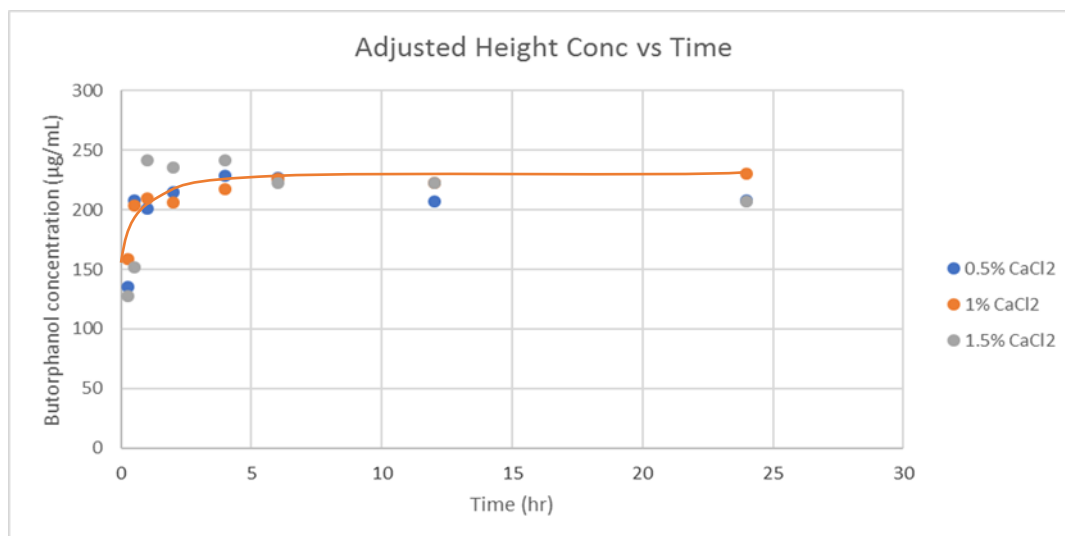
4.5.4.1 NC-SA gel release

The results showed that the hydrogel crosslinked with 1% CaCl₂ had the slowest consistent release rate in the RO H₂O with the 0.5% and 1.5% CaCl₂ having faster release rates (Graph 3, Table 5). The 0.5% hydrogel was likely the weakest matrix and when exposed to large amounts of pressure from the swelling, the matrix degraded resulting in the encapsulated drug being released.

The 1.5% CaCl₂ gel produced the densest hydrogel. This meant that the ratio of butorphanol on the surface to encapsulated within the matrix was believed to favour the surface area. This would result in the observed rapid release of the butorphanol into the solution while the physical nature of the hydrogel was largely unchanged over time.



Graph 3: Butorphanol concentration calculated from the peak height vs time for hydrogels with various CaCl₂ concentrations. The 1% CaCl₂ produced the best release rate, shown as the orange trendline.



Graph 4: Butorphanol concentration calculated from the peak area vs time for hydrogels with various CaCl₂ concentrations. The 1% CaCl₂ produced the best release rate, shown as the orange trendline.

Table 5: HPLC results from hydrogel release rates within RO H₂O with various CaCl₂ concentrations of crosslinking. Adjusted to account for the removal of the 1 mL samples and replacement with 1 mL RO H₂O.

0.5% CaCl ₂				
Hours	Area concentration (µg/mL)	Height concentration (µg/mL)	Adjusted area concentration (µg/mL)	Adjusted height concentration (µg/mL)
0.25	135	135	135	135
0.5	243	210	240	207
1	231	205	226	201
2	270	221	262	214
4	294	238	283	229
6	296	238	282	227
12	275	219	259	207
24	278	222	260	208
1% CaCl ₂ Alginate				
Hours	Area concentration (µg/mL)	Height concentration (µg/mL)	Adjusted area concentration (µg/mL)	Adjusted height concentration (µg/mL)
0.25	164	158	164	158
0.5	232	206	230	204
1	255	213	250	209
2	255	213	248	207
4	281	226	270	217
6	292	237	278	226
12	291	236	275	223
24	304	247	284	231
1.5% CaCl ₂ Alginate				
Hours	Area concentration (µg/mL)	Height concentration (µg/mL)	Adjusted area concentration (µg/mL)	Adjusted height concentration (µg/mL)
0.25	131	128	131	128
0.5	145	153	144	152
1	290	246	284	241
2	286	243	278	236
4	290	251	279	241
6	282	234	268	223
12	283	236	267	223
24	265	221	248	207

4.5.4.2 Chitosan-nanocellulose hydrogel release

The chitosan-nanocellulose gel had an almost instant release rate, the butorphanol was completely released into the solution within the first 30 minutes. This was likely due to the hydrogel matrix not completely forming. This meant that the butorphanol is released immediately and taken into the solution.

4.6 Animal trials

Broiler chickens were used as the model avian species due to their low cost, the ease of management, low maintenance requirements, high availability and prior ethical permission being already achieved. The traditional therapeutic range for butorphanol in broiler chickens is 50-80 ng/mL which is far higher when compared to other common mammalian species.³⁴

The broiler chickens were subcutaneously injected under aseptic conditions to prevent infections which may influence the serum levels or cause the animal distress. Serum samples were obtained at regular time intervals in order to determine the release rate of the drug and retention within the chicken's system.

The 6 mg/kg dosing of the chickens ensured that the chickens would not be overdosed and that the size of the chicken would not affect the overall concentration of butorphanol present in the serum. This is based on the manufacturer's guidelines for the commercial butorphanol injection recommendation. It was also assumed that the hydrogel would release the drug slower than the commercial butorphanol, or at worst the same rate as the commercial solution and therefore would not be an issue.

The chickens were provided with a constant supply of feed and water to reduce the stress on the animals and reduce the effect of diet upon the chicken serum results. The chickens were kept in a thermally stable area and had a radio playing to acclimatise the chickens to human speech and reduce the stress caused by human interaction.

The injection caused no visible inflammation (Fig 23) or discomfort to the chicken as expected due to the biocompatible nature of the hydrogel. There was a small lump present where the hydrogel had been subcutaneously injected. This was believed to be the hydrogel itself rather than any swelling or inflammation due to the lack of discolouration or excessive heat. The chickens that were injected with the commercial butorphanol (Fig 24) also showed no adverse reactions.

The lump was not present after 48 hr and was believed to have been degraded, disrupting the hydrogel matrix structure and breaking up the polymer chains. After testing had been completed the animals were euthanized as specified by the ethical permission application.

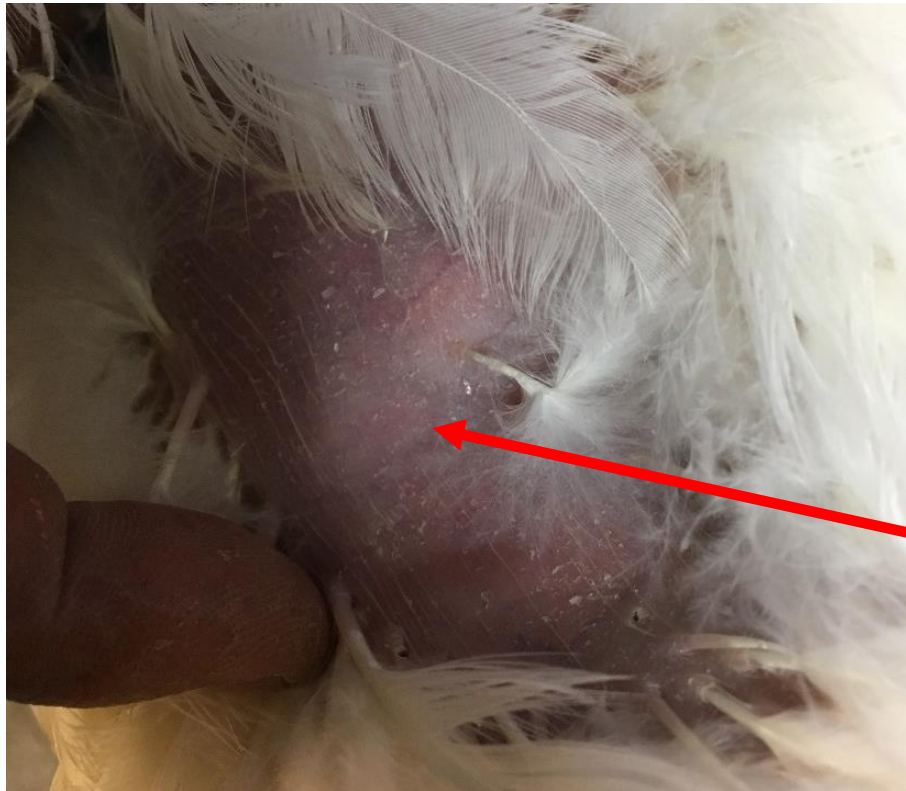


Figure 23: Chicken neck 30 min after injection with butorphanol hydrogel. The small lump present is the injected hydrogel. No inflammation was observed. Red arrow indicates injection site.



Figure 24: Chicken neck 30 min after injection with commercial butorphanol. No lump present and no inflammation observed. Red arrow indicates injection site.

4.6.1 Sample collection issues

When collecting the samples there were numerous issues encountered due to the nature of the animals examined. When inserting the catheters, the chickens were mildly distressed due to human handling. This resulted in complications such as the animal kicking out before the catheter could be secured to the leg, knocking out the catheter and damaging the veins. Subsequent catheters then had to be implanted into the alternate leg or abandoned for manual blood sampling.

There were also difficulties extracting blood samples. The catheter was sometimes compressed or bent preventing blood flow. The heparin generally prevented clotting within the catheter and allowed easy extraction of the blood but occasionally there would be a blood clump formed that blocked the catheter.

After collection had begun, the catheter could no longer be replaced; it would require professional assistance and would increase the risk of harming the chicken. If the catheter was knocked loose the subsequent blood samples were taken by direct injection of the needle into the veins in the leg. This was performed by Aline Alberti Morgado.

The centrifugation step was to remove unwanted components of the blood such as haemoglobin and fibrin clots while leaving the serum containing butorphanol unaffected. However, the nature of the blood samples changed depending on the stress levels of the animal, resulting in vasoconstriction, this increased the blood pressure. This caused some blood samples to contain different levels of haemoglobin, this meant that the same amount of blood sample to have proportionally less serum. This resulted in some samples containing less serum and therefore reduced the amount available for subsequent testing.

This problem was reduced by taking a larger volume of blood but this required larger broiler chickens to be able to tolerate the associated blood loss. The larger birds were considerably obese and were therefore more prone to health problems associated with their weight and the stress of handling. This also resulted in the death of a total of three chickens before and during the testing process, one of which perished before any treatment had been applied.

4.7 Serum analysis

The *pilot* study chicken serum samples provided for analysis and the samples extracted as part of the *primary* study were not always uniform. The volume of serum, colour and consistency varied dramatically for the supplied samples from the *pilot* study. The *primary* studies samples were relatively uniform with some mild variation in the volume and colouration.

Samples from both studies were occasionally contaminated with small amounts of blood, shown by a darker red/brown coloured serum. Other serum samples were clear but had a large clear solid, believed to be a fibrin clot produced by amalgamation of residual amounts of fibrinogen present after centrifugation.

The *pilot* study samples had problems with clotting reducing the volume of usable serum. This prevented the overall SPE extraction being done in duplicate for all of the supplied samples. There were also some samples that were not supplied due to them being misplaced or the chicken's catheter being removed by the chicken's actions. This meant that a detailed release rate could not be achieved using HPLC.

This was improved in the *primary* study where a larger amount of blood was removed to increase the amount of available serum. There were also improved collection techniques used. These included taking care not to disturb the pellet after centrifugation when removing the serum. This reduced the presence of blood in the serum and maintaining a cold temperature of the samples before freezing at -20°C prevented degradation of the butorphanol levels in the samples.

4.8 HPLC

4.8.1 SPE

The SPE cartridge extraction was performed under vacuum suction in order to reduce the hands-on time requirement. Without suction, the drip rate was roughly 1 mL/min and increased the risk of contamination due to long term exposure to the air (≈ 1 hr total exposure).

The RO H₂O was added to dilute the plasma samples. This reduced the amount of initial serum required as the SPE cartridges function ideally with ≈ 1 mL of solution.

This also made it possible for blank serum samples to be spiked with known concentrations of butorphanol, replacing the RO H₂O yet not altering the final volume of solution loaded into the SPE cartridges.

The 2 M HCl was added to lower the pH of the solution, disrupting the binding of butorphanol to the various components of the serum.⁵⁸ This allowed the butorphanol to be released into the solution as free butorphanol. The free butorphanol could then bind to the SPE cartridge.

The drying of the cartridge after each wash step ensured there was no solution present in the cartridge which could alter the elution of the desired product or interfere with the subsequent wash step.

The butorphanol was eluted with 100% methanol, disrupted the binding of the butorphanol to the SPE cartridge and releasing the butorphanol into solution. The solution was then collected into test tubes and dried under vacuum centrifugation to remove the methanol. This reduced the risk of contamination from methanol or remaining solvents that may change the peak height, area or retention time. The dried butorphanol was then reconstituted in mobile phase to prevent further contamination.

4.8.2 HPLC Run Protocol

A reverse phase C18 column was used because the butorphanol is less polar than the mobile phase, this increased the retention time of the butorphanol, allowing it to be separated from the other peaks evaluated at 202 nm. The temperature was increased to 40°C as the nature of the mobile phase was causing high pressure in the column. This is because salts were precipitated and deposited onto the guard and HPLC columns at lower temperatures.

This precipitation of salts caused clogging in the columns which required longer washing steps to remove. It would also occasionally cause the machine to shut down during longer runs making it impossible to run multiple chickens' samples without running the cleaning protocol. The increased temperature also decreased the retention time, the higher pressure caused the butorphanol to be released sooner. By lowering the pressure, the butorphanol remained bound for longer and produced a clearer, more isolated peak.

The HPLC column allowed separation of the butorphanol peak from the other compounds present in the blood without requiring an expensive mobile or solid phase. The column could be cleaned quickly and thoroughly to prevent carryover from previous experiments which may corrupt further results.

The samples were kept in sealed HPLC vials at 4°C to reduce the risk of the sample degrading while waiting to be run. This decision was made based on previous publications which showed temporary storage at refrigerated temperatures ($\approx 4^{\circ}\text{C}$) did not have adverse effects on the reconstituted sample of volatile substances.

It was therefore assumed to have either a non or a limited effect upon the SPE treated plasma samples.⁵⁹

The wavelength used to analyse the samples was chosen to be 202 nm. Other absorbances' did have a larger butorphanol absorption peak but there were other peaks present at similar retention times. 202 nm was chosen as it provided the greatest definition of the butorphanol peak without the interference of unwanted peaks.

These interfering peaks could corrupt the results by artificially increasing or decreasing the peak area or height.

The phosphate buffer used was similar to the buffer used in previous chicken butorphanol analysis studies³⁴ with the exception of lowering the pH to 4. This lowering of the pH reduced the amount of salt that precipitated on the column.

These changes also caused the butorphanol peak retention time to increase from ≈ 13 min in the previous study³⁴ to ≈ 14 min, separation of the peaks present in the mobile and the plasma was also more effective. The buffer had the pH balanced with the minimal amount of NaOH. This was done because the NaOH produced a small peak at a similar retention time to the butorphanol peak.

As long as the amount of NaOH was very low, the peaks remained distinct and the butorphanol peak could be integrated with a high degree of accuracy.

4.8.3 HPLC Analysis

Injections of the chickens with the gel and commercial butorphanol solution was performed to provide context for the experimental results. The commercial formulation release rates were used as a baseline for determining the hydrogel release rate.

Examining the absorption and degradation rate of the commercial butorphanol could also be used to compare with the release rate of the butorphanol from the hydrogel into the chicken's system.

The butorphanol concentration of the serum samples was based upon the standard curve constructed from the butorphanol standard curve.

By performing this experiment on a large sample size (6 chickens), the effect of the variations in the broiler chicken's metabolisms was minimised. This allowed for percentage variations to be calculated with a higher degree of accuracy and the ability to identify and discard any outliers.

When performing the *pilot* study, the samples were run in duplicate after SPE. This reduced the uncertainty for the samples but due to the lack of serum samples multiple SPE runs were not possible for the *pilot* study serum samples.

This was deemed unnecessary as previous studies by Dr Preet Singh had found negligible variation in the SPE extractions.³⁴

The *primary* study samples were run in duplicate after SPE had been performed in order to minimise uncertainty. However, there was enough serum sample to rerun any results that differed dramatically from the expected results allowing for a far greater confidence in the results. Any outlier could be identified, re-tested and upon further testing produced results that agreed with the other samples.

The variation in HPLC results was occasionally caused by spikes in pressure as the guard column became clogged due to precipitation of salts or small molecules falling into the test tubes. This reduced the retention time, causing the butorphanol peak area and height to change as the HPLC run continued. This made the known concentration solutions of butorphanol impossible to determine so the samples were prepared again and rerun.

The HPLC column was replaced after the samples from the *primary* study showed that after 4 chicken gel samples and 5 chicken no-gel sets had been run and dramatic variations in peak height and area were observed.

The new column had lower inter and intraday variation when the samples were re-run and used for the final analysis.

4.8.4 New column

This showed recovery rates of butorphanol similar to those reported³⁴ and retention times that separated the butorphanol peaks from other, undesired peaks present near the end of the experimental run. The retention time was larger than the previous column and other reported times by roughly 1 minute but this is believed to be a result of the lower pH buffer used in the mobile phase and was considered acceptable.

4.8.5 HPLC cleaning protocol

The initial wash step involved removing the guard column and running RO H₂O with high pressure to remove any water-soluble compounds present on the guard column. The HPLC column was then reattached and washed with a lower pressure run that lasted 30 min to remove any remaining water-soluble compounds. These included any precipitated salts remaining on the column which could interfere with subsequent runs.

The 50:50 acetonitrile:RO H₂O cleaning solution was sonicated for 10 min to remove any air bubbles that may be present after the mixing step before being used in wash steps. These bubbles would otherwise have been taken into the feedlines and potentially would cause problems with the column by altering the column pressure and introducing more peaks in the UV analysis.

The final cleaning step was run for 30 min to remove any remaining contaminants and prepare the HPLC column for temporary storage without the risk of damage to the column membrane. The water:acetonitrile mixture was used for short term storage and 100% acetonitrile would be used before prolonged storage (3+ months)

4.8.6 HPLC sampling problems

Inconsistencies with the 8 hr gel samples were believed to be caused by the needle calibration for the sample tray being off for the sample vials. This error occurred only in the 8 hr gel samples as the no-gel samples were loaded into a separate column on the sample tray when the HPLC runs were performed.

Occasionally the sampler needle would not inject correctly into the vial, striking the edge of the glass insert and damaging the vial insert or causing the machine to automatically shut down, this then required longer cleaning times and the sample preparation to be repeated. To prevent this from reoccurring the final two vial slots in each column were never used and from then on, no dramatically different results were observed for the 8 hr gel samples.

The HPLC needle was also found to be bent and not taking up a consistent volume from the vials resulting in a large variation within the replicates of the samples. This helped to explain the large variation that had been present in the samples from the pilot study. This meant that the samples had to be repeated to reduce the variation. The samples analysed before December 2018 were therefore re-run with the new HPLC column and analysed.

4.9 HPLC validation

4.9.1 HPLC linearity

The butorphanol standard curve showed that the butorphanol peaks produced by HPLC had a linear relationship to the concentration within the 1 µg/mL to 15.6 ng/mL standard curve (Graph 7). This relationship was reproducible with minor variation so it was decided that the samples only required 3 standards per run to reduce run times. The 15.6 ng/mL sample had a greater degree of variation but was still within the acceptable range to produce a linear standard curve (Graph 5).

The retention times of the butorphanol peak had a variance of ≈ 0.2 min (Graph 8, 9)). The longer the run was, the smaller the retention time became as the sedimentation of salts on the guard column caused minor increases in the pressure ($\approx 0.1 - 0.2$ mpa). The increased pressure caused the butorphanol to be released from the column faster, resulting in the lower retention time.

The inter sample standards were used to determine if there was any change in the peak area and height during the experimental runs. They concentrations chosen were 500, 250 and 125 ng/mL standards of butorphanol in the mobile phase. These standards were within the middle of the expected range for the chicken samples and could be extrapolated to calculate the concentration of butorphanol present in each sample. The standards used were above the minimum effective dose of 50-80 ng/mL.

Any serum concentrations which were lower than the effective dose were not considered vital. The standards run during sampling were compiled to calculate the average peak area and height then graphed to determine to determine the linearity of the relationship. The R^2 value of 1 (Graph 5,6) showed that the peak area and peak height of the butorphanol standards had a linear relationship to the concentration. This showed that the relationship was consistent and could therefore be trusted for use in determining the butorphanol concentration in the chicken serum samples.

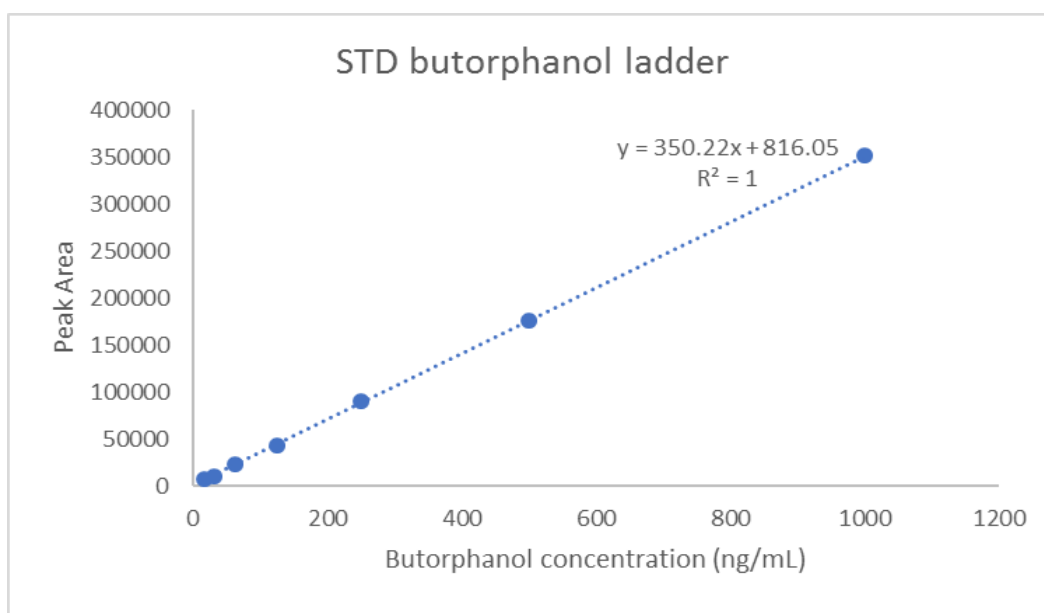
4.9.2 HPLC specificity

The inter-day variances were calculated (Table 4) and showed that there was very little variation present. Any variation was likely a result of the pressure changes which generally occurred as more samples were run.

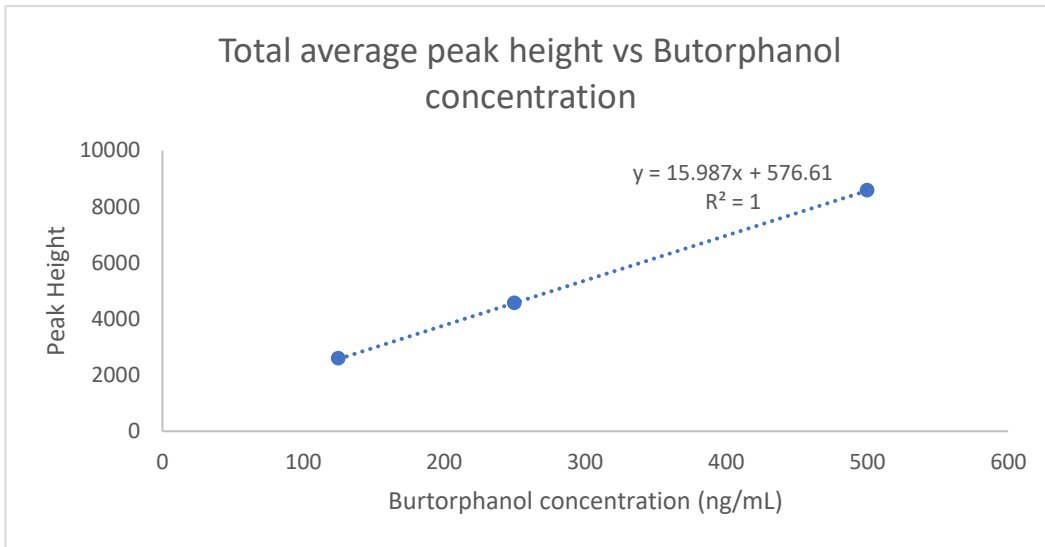
The intra-day variation was determined and showed that there was a very low variance (Table 6). This reinforced the idea that the serum results from different days could be trusted to contain limited variation.

Table 6: Intra-day variation of butorphanol standards including percentage variance and average areas with heights. The low variance values show that there is little variation between the standards run on different days.

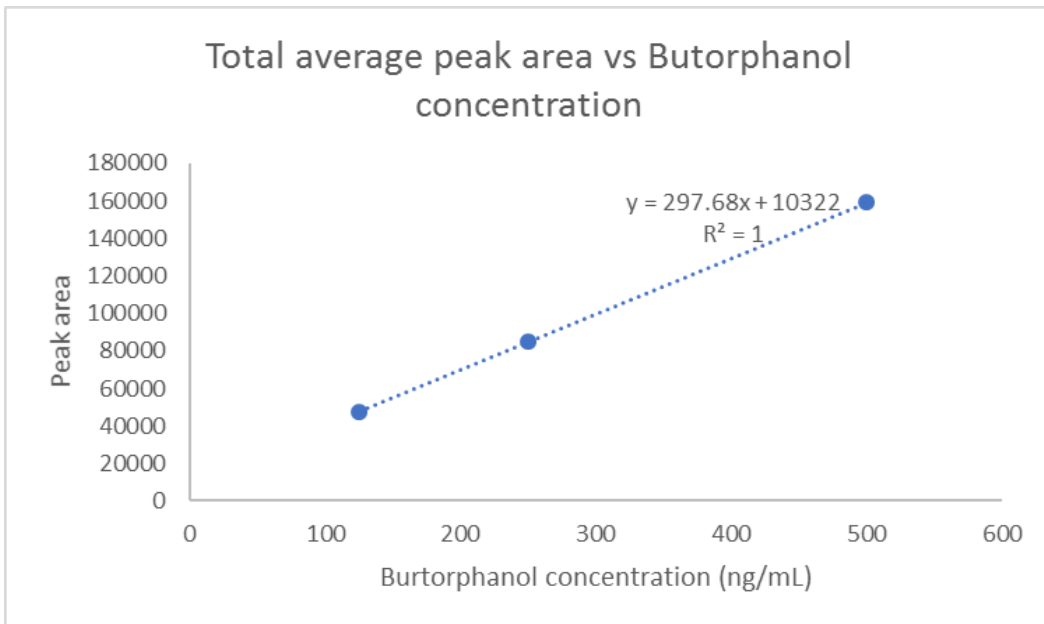
Standard	Average Area	Average Height	Area variance	Height Variance	Area variance %	Height Variance %
125 ng/mL	$4.31 * 10^4$	$2.37 * 10^3$	55.0	3.30	0.127	0.141
250 ng/mL	$8.81 * 10^4$	$4.74 * 10^3$	335	17.0	0.379	0.359
500 ng/mL	$1.75 * 10^5$	$9.41 * 10^3$	224	15.3	0.128	0.162



Graph 5: Butorphanol stand curve for 125 ng/mL 250 ng/mL and 500 ng/mL vs HPLC peak area.

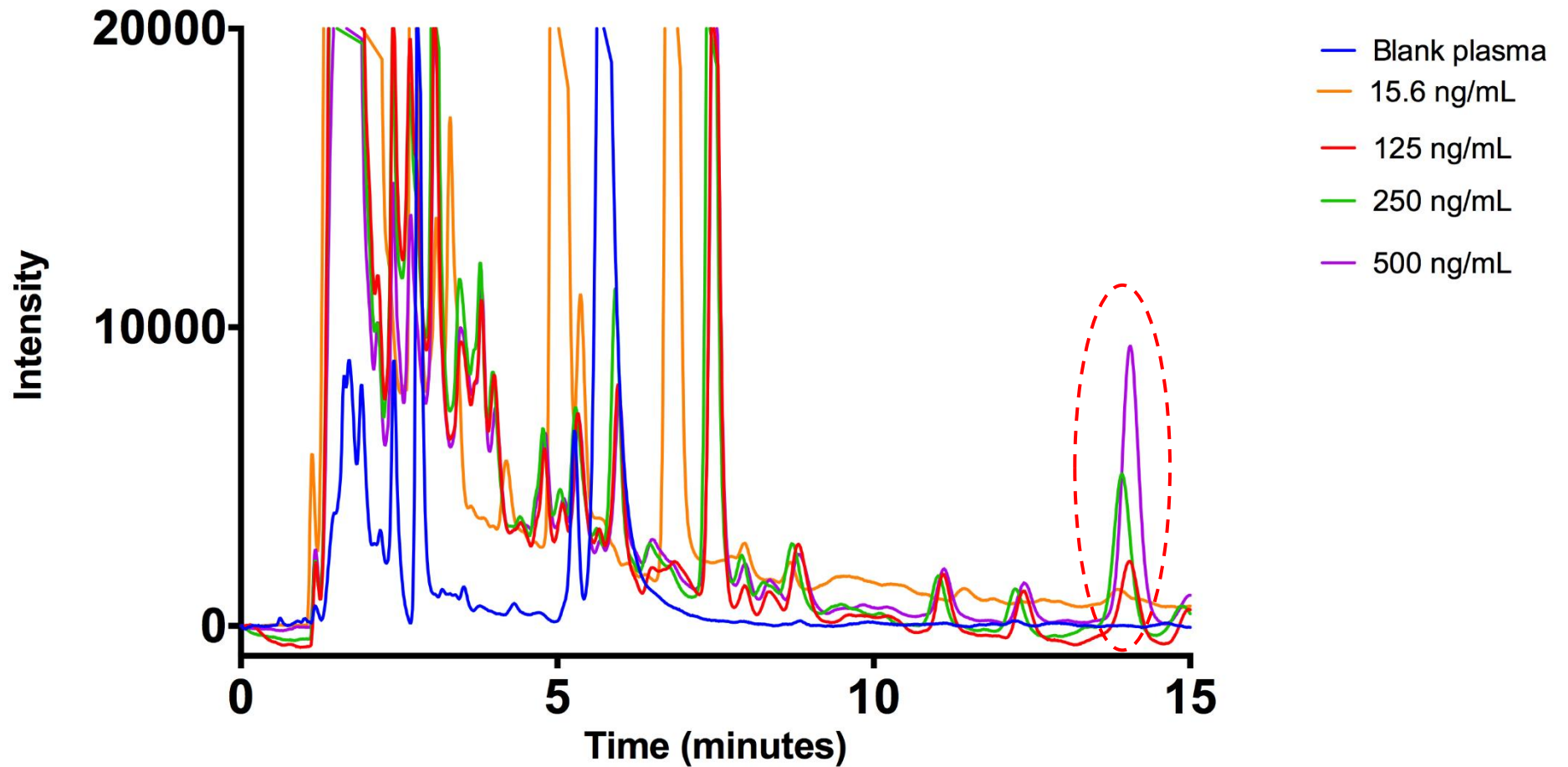


Graph 6: Butorphanol stand curve for 125 ng/mL 250 ng/mL and 500 ng/mL vs HPLC peak height.



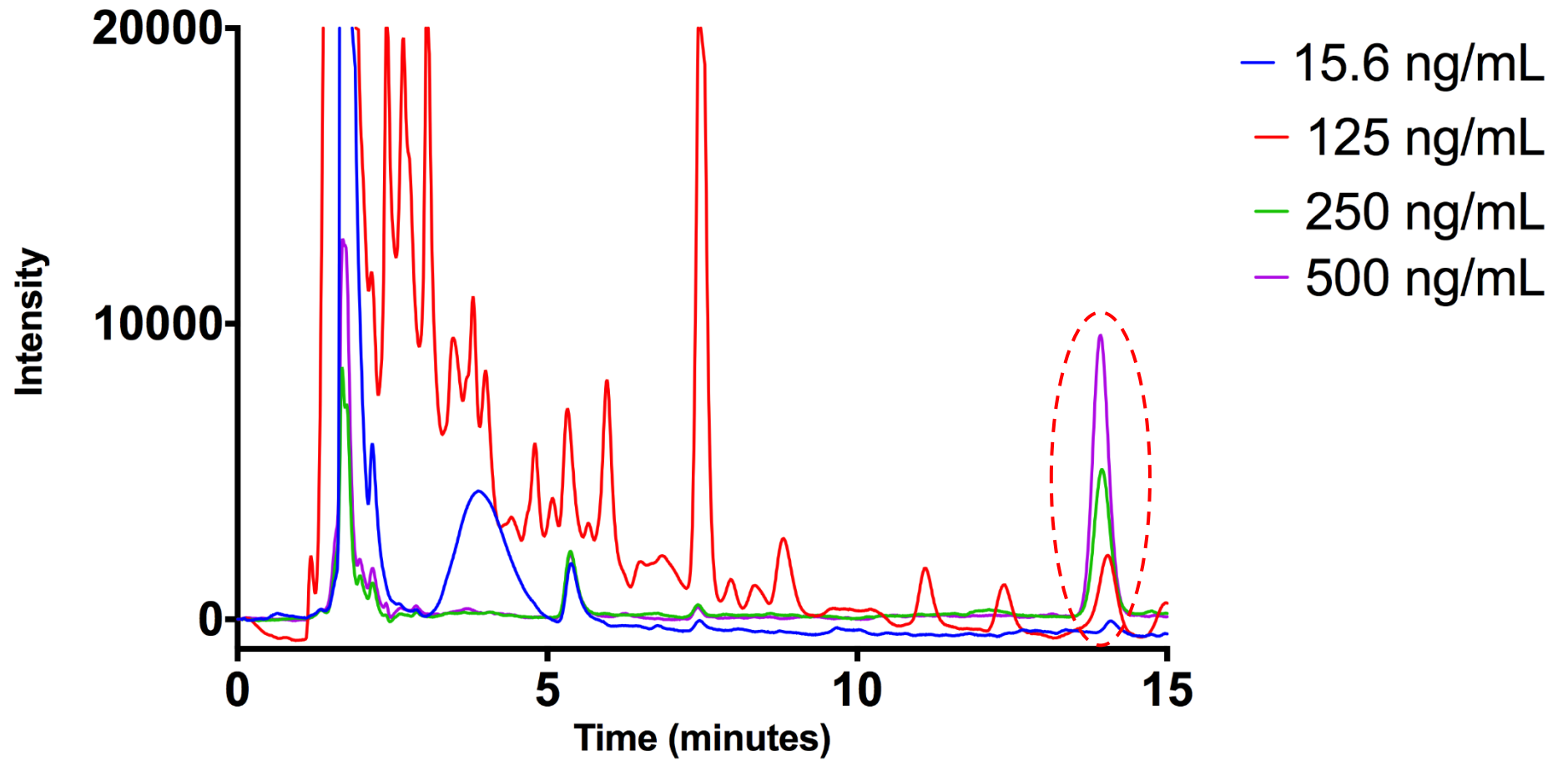
Graph 7: Butorphanol standard curve 15.6 ng/mL → 1 mg/mL, concentration vs HPLC peak height.

Spiked plasma



Graph 8: Chromatograph of four butorphanol spiked plasma standards and blank plasma. The area highlighted is the butorphanol peak. Minor variations in pressure resulted in slightly different retention times. The higher intensity of the 15.6 curve was due to sedimentation of salts within the column but the peak area was within the expected range.

Standards



Graph 9: Chromatograph of the three butorphanol standards in mobile phase. The area highlighted is the butorphanol peak. Minor variations in pressure resulted in slightly different retention times.

The blank plasma samples and a sample of mobile phase were run at the beginning of every chicken sample run to ensure that there was no carryover from previous runs or peaks occurring with the same retention time as the butorphanol peak. The results showed that the majority of blank plasma and mobile phase runs had no peaks present. The few samples that did had very small peaks.

When the column was re-washed and the samples re-run, no extraneous peaks were present. This indicated that there could be some carryover but the risk was very low and the effect on the final results was determined to be negligible.

The experimental results (Graph 8,9) show that the lower limit of quantification for the butorphanol standards and spiked plasma samples was 15.6 ng/mL.

4.10 Primary Study

4.10.1 Gel release rate

The gel release rates were determined from analysis of the chicken serum samples using SPE and HPLC. The gel release rate HPLC results had to be further processed to produce an accurate reading for the butorphanol level in the sample. The samples were dried and then reconstituted so even if the recovery rate from the SPE cartridges was 100% and there was no loss during the processing steps. The final concentration will be higher as the original 300 μ L of sample were reduced to a 200 μ L final volume.

The hydrogel was also suspended in commercial butorphanol and swelled to encapsulate the drug. However, this resulted in the concentration in the hydrogel being lower than the commercial solution due to a supernatant dilution factor caused by the hydrogel itself. This potentially caused the lower concentrations of butorphanol recorded at 15 min, 30 min and 1 hr when compared to the commercial solution.

The gel release rates were based on the average of all consistent serum samples from the chickens injected with the butorphanol hydrogel and the commercial butorphanol solution.

After subcutaneous injection, the butorphanol was either released into the tissue from the hydrogel or was already present as a stock solution. It then passed through the chicken's muscle tissue and was taken up into the blood supply.

The release rates show that in the initial time points (15 min, 30 min, 1 hr) the commercial solution was released into the blood supply at a far higher rate than that of the hydrogel (Graph 10, 11).

This is because the hydrogel must release the butorphanol from the gel matrix into the surrounding tissue before it can pass into the blood stream, therefore lowering the uptake rate.

After 1 hr, the serum samples from the chickens injected with the hydrogel had higher butorphanol levels within their serum than the chickens injected with the commercial butorphanol solution. After 4 hrs had passed the serum levels from the commercial injection had dropped below the minimum effective dose level (Graph 12).

The chickens injected with the hydrogel had a butorphanol level remaining above the effective dose level up to 26.5 hrs where the level then dropped below the minimum effective dose level and was no longer deemed effective.

4.10.2 Pharmacokinetic analysis

Pharmacokinetic parameters were determined using noncompartmental analysis (Table 7,8). The elimination rate constant (λ_z), maximum plasma concentration (C_{max}), time to achieve C_{max} (T_{max}), half-life ($t_{1/2}$) and clearance of drug (Cl/F) were determined directly from the plasma concentration data. The area under the curve (AUC) and the area under the first moment (AUMC) were determined using the linear trapezoidal method. Mean residence time (MRT) was calculated as $AUMC/AUC$.

The elimination rate constant is a pharmacokinetic term referring to the rate the drug is removed from the system. The average results showed that the λ_z level was higher for the NG samples when compared to the gel samples (0.77 1/hr vs 0.06 1/hr). This suggested that the gel continued to release the drug over a far longer period than the commercial butorphanol. The drug was removed via degradation within the liver and absorption into the cerebral and spinal tissue.

The half-life of butorphanol is the time when the concentration of butorphanol in the serum is half the maximum concentration (C_{max}). The half-life within the system is far higher in the serum samples from the chickens injected with the hydrogel (12.25 hr vs 1.5 hr). The higher half-life correlates with the slower release rate of the butorphanol from the hydrogel.

As the release rate from the hydrogel decreases with time, the systems breakdown of the butorphanol would be able to catch up. This reduces the total amount of butorphanol within the system producing the observed half-life.

The T_{max} was the time in hours it took to achieve the maximum concentration within the serum samples (C_{max}). There was little observed difference between the T_{max} averages from the chicken serum samples (0.5 hr gel vs 0.4 hr no gel). This indicates that the T_{max} is primarily influenced by uptake from the subcutaneous tissue to the blood stream. The minor increase in T_{max} time from the gel sample was likely caused by the hydrogels release rate.

The C_{max} is the maximum observed concentration (ng/mL) and was very similar between the gel and no gel serum samples. This suggested that the hydrogel contained a large amount of butorphanol on the peripheries where it could be easily released. The butorphanol was then absorbed into the blood stream at the same rates producing the similar maximum concentrations within the serum.

The area under the curve (ng/mL * h) showed that the gel samples had a higher average concentration of butorphanol within the serum over the measured time period (5893 vs 1449). The area under first moment (ng/mL * h²) exhibited similar results (6438 vs 1513) with the gel serum samples again producing the larger value.

The area under the curve from 0 to infinity is the total area under the graph from time 0 till infinity (ng/mL * h) and the area under the main curve to infinity is the total area under the main curve from time 0 to infinity (ng/mL * h).

The mean residence time MRT (h) is the average amount of time a drug molecule remains within the system. It is calculated from the sum of all the residency times divided by the number of drug molecules.

The clearance of drug (mg)/(ng/ml)/h is the rate the active drug is removed from the body. It is the rate at which the drug is eliminated divided by the plasma concentration of the drug. This is generally a constant rate. The hydrogel serum samples had a lower clearance rate (0.005 vs 0.016) which helped to explain why the butorphanol level within the serum remained above the minimum effective dose for a longer time.

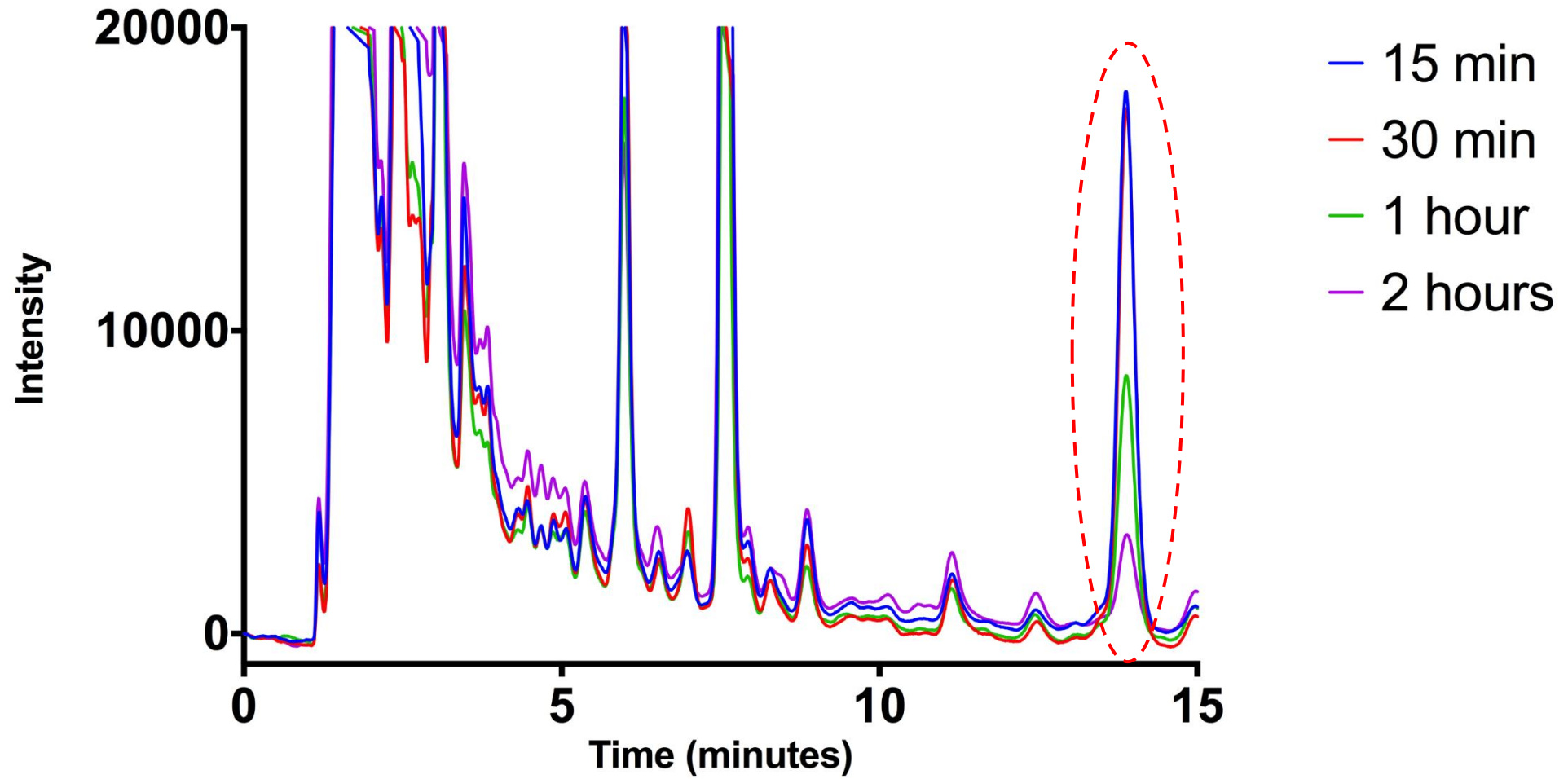
Chicken	Units	Gel 1	Gel 2	Gel 3	Gel 4	Gel 5	Gel 6	Average	Variation	Variation %
Lambda_z	1/h	0.057160089	0.10123133	0.0566255	0.0566255	0.032949322	0.07718589	0.063629605	0.00702	9.93
t _{1/2}	h	12.12641876	6.847160679	12.24090182	12.24090182	21.03676587	8.980231764	12.24539679	1.59	11.5
T _{max}	h	0.5	0.25	0.5	0.5	1	0.5	0.541666667	0.0929	14.65
C _{max}	ng/mL	553.97	1086.812	1225.408	1225.408	1479.854	1221.49	1132.157	71.05	5.90
AUC 0-t	ng/mL * h	1679.269115	2073.944318	4778.329545	4778.329545	14890.83075	7162.46187	5893.860856	3319.79	36.03
AUC 0-inf_obs	ng/mL * h	1921.501241	2238.802174	5585.294258	5585.294258	15761.79039	7535.854209	6438.089421	3303.89	33.9
AUMC 0-inf_obs	ng/mL * h ²	16695.95116	23780.15676	61712.96966	61712.96966	493036.9925	73206.56528	121690.9342	230164.79	65.4
MRT 0-inf_obs	h	8.689013986	10.62182136	11.0491886	11.0491886	31.28051956	9.71443492	13.73402784	4.53	24.8
Cl/F_obs	(mg)/(ng/mL)/h	0.010304443	0.008844015	0.003974723	0.003974723	0.001484603	0.002866297	0.005241468	0.00196	27.2

Table 7: Summary of pharmaceutical analysis of Chickens treated with the hydrogel in the *primary* study.

Chicken	Units	NG 1	NG 2	NG 3	NG 4	NG 5	NG 6	Average	Variation	Variation %
Lambda_z	1/h	1.92931204	1.100915569	0.562644864	0.409434766	0.406853261	0.230625614	0.773297686	0.442	36.4
t _{1/2}	h	0.359271681	0.629609754	1.231944384	1.692936793	1.703678566	3.005508233	1.437158235	0.516	26.4
T _{max}	h	0.25	0.5	0.5	0.25	0.5	0.25	0.375	0.0417	10
C _{max}	ng/mL	1833.413	1146.854	1192.335	776.5288	1207.245	676.3906	1138.7944	122.23	9.69
AUC 0-t	ng/mL * h	1653.885425	1490.84368	1495.39657	1275.137953	1611.373565	1168.186553	1449.137291	20.86	1.42
AUC 0-inf_obs	ng/mL * h	1699.487535	1514.129326	1651.857467	1325.487414	1661.795626	1228.662359	1513.569954	21.16	1.38
AUMC 0-inf_obs	ng/mL * h ²	1190.295019	1577.121061	2640.703632	2792.917078	2599.138582	4070.343921	2478.419882	346.03	12.25
MRT 0-inf_obs	h	0.700384672	1.041602612	1.598626809	2.107086834	1.564054292	3.31282544	1.720763443	0.409	19.22
Cl/F_obs	(mg)/(ng/mL)/h	0.014474952	0.016643228	0.014529099	0.019464538	0.014803264	0.019045102	0.016493364	0.000264	1.58

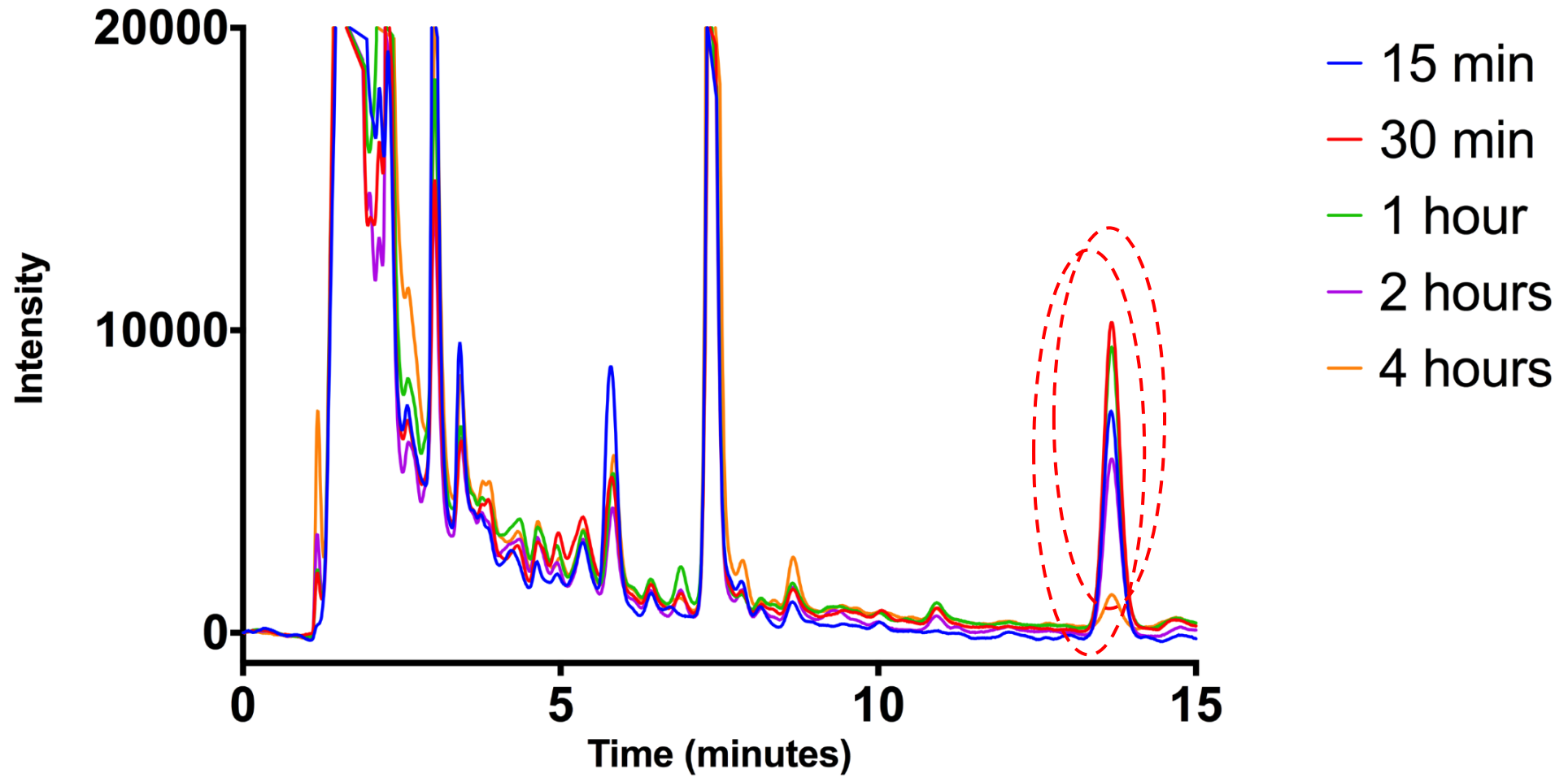
Table 8: Summary of pharmaceutical analysis of 6 of the Chickens treated with the commercial butorphanol in the *primary* study that had the lowest variation.

No Gel Chickens

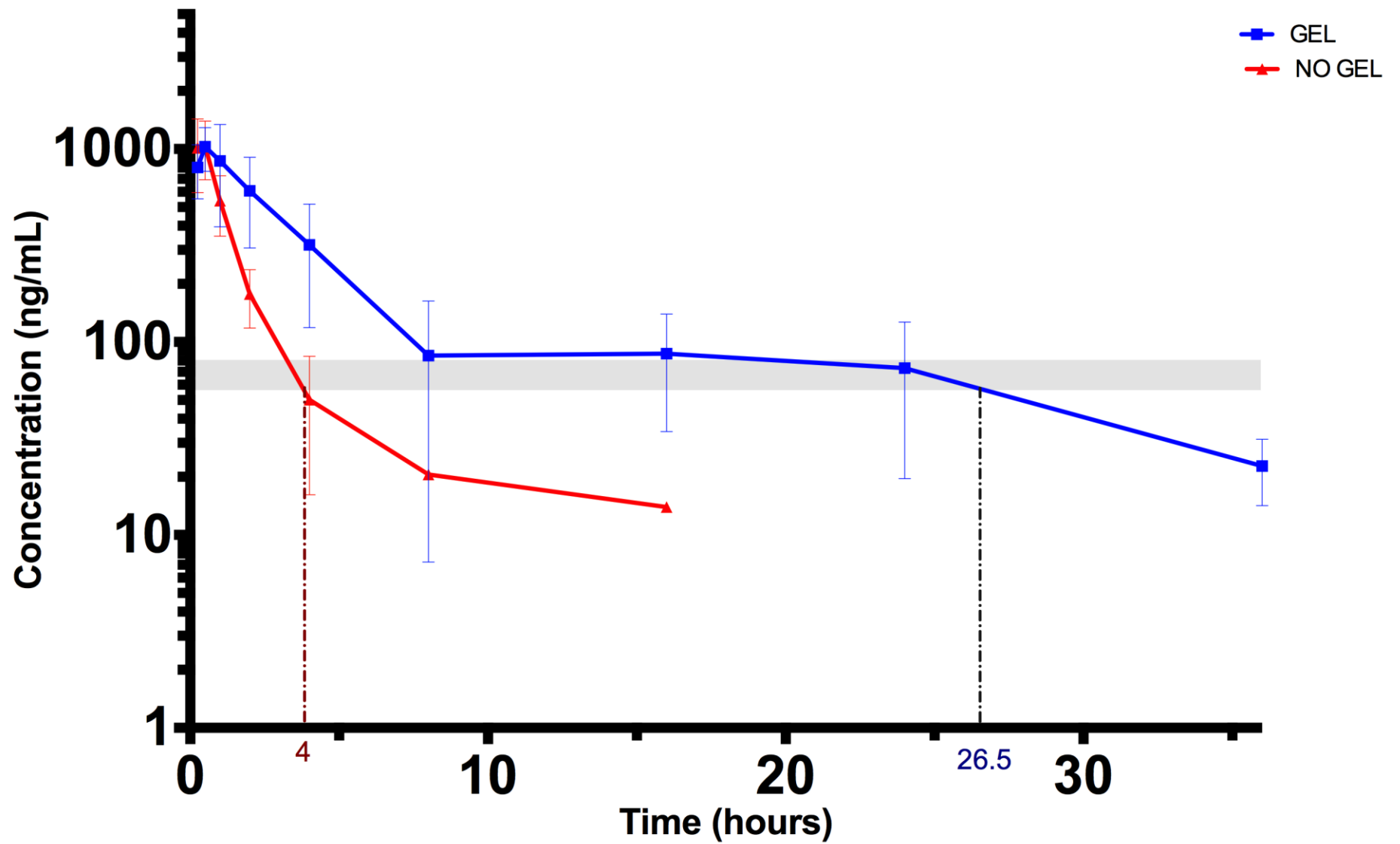


Graph 10: Chromatograph of serum from the chickens injected with commercial butorphanol. The area highlighted is the butorphanol peak.

Gel Chickens



Graph 11: Chromatograph of serum from the chickens injected with the NC:SA hydrogel. The area highlighted is the butorphanol peak.



Graph 12: Semi-Log graph comparing the butorphanol concentration of the serum samples over time. The blue is the serum results from the 6 chickens injected with the 3% m/V 1:9 NC-SA 1% CaCl₂ hydrogel. The red line is the serum results from the 6 chickens injected with commercial butorphanol. The shaded area is the range for the minimum effective dose (50-80 ng/mL). The error bars show the standard deviation.

5. Conclusion

The original aims of this project were to produce cellulose at a nano scale and then develop a hydrogel. This hydrogel would be based upon a composite of crosslinked nanocellulose monomers and traditional hydrogel materials. The first year primarily focused upon production of nanocellulose from hemp fibres and *G. xylinus* in preparation for hydrogel production and analysis.

The microfibrilated cellulose was successfully extracted from the hemp fibres and then TEMPO oxidised to form nanofibrilated cellulose. The cellulose contained carboxylate groups, ideal for crosslinking interactions. The bionanocellulose was produced from *G. xylinus* but the yield was considered too low for further hydrogel production.

The hydrogels were then produced from various ratios of nanocellulose and traditional hydrogel materials. This was done to determine the ideal composition for swelling and release of encapsulated drugs. The water release rates showed that the hydrogel required nanocellulose to stabilise the gel matrix when suspended in RO H₂O.

Chitosan was briefly examined but was not explored in detail due to the limited time available. The pure chitosan hydrogel lacked the mechanical stability when submerged in RO H₂O, even when crosslinked with CaCl₂. Composite crosslinked hydrogels composed of chitosan and nanocellulose had release rates of butorphanol in RO H₂O that were too high for prolonged drug treatment.

The ideal composition was found to be a 3% m/V 1:9 NC:SA hydrogel that had been crosslinked with 1% m/V CaCl₂. This hydrogel could swell to a large extent, without breaking up the hydrogel matrix. The release rate of encapsulated butorphanol was also lower and more consistent than that of the other compositions.

Once the ideal hydrogel had been identified and produced, in-vitro testing in chickens was conducted. This was the primary focus of the second year. The hydrogel was compared to a solution of commercial butorphanol that had an identical concentration and was injected in the same manner. The chickens were of very similar age and weight. They were kept in identical conditions to minimise any deviations caused by environmental conditions.

The in-vivo testing showed very promising results. The hydrogel treated chickens had a butorphanol serum level capable of producing an analgesic effect for 26.5 hrs. This was compared to the commercial solution which had the butorphanol level drop below the effective dose after 4 hrs had passed.

When this is compared to the alternative delivery mechanisms detailed in 2.6.2.2, the hydrogel has overcome many of the existing problems. The hydrogel is easily injected and rapidly begins to release butorphanol into the system, inducing an analgesic effect within 15 min which is preferable to the 6-12 hrs required by the osmotic pumps. The analgesic effect lasted far longer than the effect produced by the polyoxomer gel and the preparation was less intensive than the liposomal formulation.

Overall the aims of the project had been achieved and surpassed with in-vitro and in-vivo analysis of the produced nanocellulose based hydrogel conducted. The results showed that the desired release rate of butorphanol had been achieved with further avenues of research discovered.

6. Future Work

The results of this thesis have shown that NC-SA hydrogels present possibilities for prolonged drug release in chickens when administered subcutaneously. The release rate was lower than the commercial butorphanol for the first hour, yet maintained a release rate at the required level for an analgesic effect for a longer time. The amount of butorphanol present in the serum over the initial time periods was low which means the initial concentration of butorphanol in the hydrogel could be increased without risking overdosing the chicken.

Increasing the concentration of butorphanol within the hydrogel may improve the release rate time if the butorphanol remains encapsulated in the hydrogel matrix. This would result in a higher butorphanol level within the serum producing an analgesic effect for a longer time period.

The hydrogel composition was restricted by the viscosity of the hydrogel and the availability of nanocellulose fibrils. The nanocellulose content of the hydrogel could be increased to examine the release rate of hydrogels that possess a higher ratio of nanocellulose to sodium alginate. The increase in nanocellulose content could then alter the required amount or nature of crosslinking.

This may alter the viscosity of the solution allowing higher concentration hydrogels to be injected or the release rate of different drugs to be altered.

The project focused on nanocellulose with sodium alginate hydrogels due to the time and resource restrictions. However, there is evidence in the literature that nanocellulose/chitosan blend hydrogels can be used for drug delivery and therefore could present a potential further avenue of research.

The nanocellulose/chitosan hydrogel produced in the project showed limited promise as the butorphanol release rate with CaCl_2 crosslinking was very high. This avenue was not explored as the NC:SA hydrogel showed a superior butorphanol drug release rate and mechanical stability so was seen as the more promising hydrogel.

Another potential research avenue is to alter the crosslinking agent to increase the strength of the hydrogel matrix while maintaining a viscosity suitable for injection. The project used CaCl_2 as a crosslinking reagent. The Ca^{2+} ions crosslink the carboxyl groups present on TEMPO oxidised nanocellulose and sodium alginate.

This means that other ions such as Mg^{2+} from MgCl_2 could be used as a crosslinking reagent, the different ion size may allow the monomers to be crosslinked more closely together. This would reduce the pore size of the hydrogel limiting the swelling profile and increasing the density, this could produce a more stable hydrogel with a lower release rate but may also prevent the uptake of larger drug molecules.

Chemical crosslinking through hydrolysable or metabolisable chemicals could also be considered such as using amides or ester groups. This would produce a far more rigidly structured hydrogel matrix and could provide more research opportunities for crosslinking reagents. The chemicals must be biodegradable and not induce an immune response by the target animal.

The final potential change to the hydrogel itself is to alter the pH of the solution, many smart hydrogels exhibit different swelling profiles dependant on the pH of the solution. Increasing the pH would reduce the amount of available carboxyl groups, reducing the strength of crosslinking and mechanical strength. Lowering the pH would increase the crosslinking strength but may cause the hydrogels to extract, expelling the encapsulated drugs.

By altering the pH of the hydrogel or injecting into areas which have a different pH, the release rate of the hydrogel could be altered to maximise the efficiency of release.

Ideally the hydrogel would be tested on a larger variety of avian species to determine its viability for veterinary treatments. The chickens provided a strong groundwork for the idea of the hydrogel as a prolonged treatment for avian pain. The various metabolisms of different bird species upon the hydrogel was not investigated and would present the most likely future for in-vivo studies. If the results were similar over multiple avian species, expanding the treatment to mammals would be the next logical step.

The non-selective uptake nature of the hydrogels allows for the potential for other opioids or water-soluble drugs to be loaded into the hydrogel. This makes nanocellulose hydrogels a good candidate for alternative drug release strategies with the other drugs also being capable of altering the release rates and release time of the drug.

This potentially makes the hydrogel suitable for delivery of other drug species with greater efficiency than butorphanol, especially drugs that were capable of binding to the nanocellulose or sodium alginate backbones directly. This binding would reduce the release rate of the drug allowing larger concentrations to be added safely to the hydrogel without risking overdosing.

The possibility of loading more than one drug into the same hydrogel could make dual therapy possible without requiring multiple injections or administration strategies. This would reduce the risk of infection and minimising the discomfort on the patient in addition to the amount of hands on time required by trained professionals for administration.

One of the primary alternative drugs under consideration was salicylic acid, a non-steroidal anti-inflammatory drug. Combining the salicylic acid with an opioid could provide treatment for arthritic pain. The salicylic acid would reduce the inflammation placing pressure upon the joints and the opioid would reduce the discomfort experienced.

Nanocellulose composites could potentially be used for long term pain release in mammalian species. The non-toxic nature of the hydrogel and wide variety of potential loading drugs makes treatment of numerous conditions possible.

The possibility also exists for nanocellulose composite hydrogels to be used for treatment of people suffering from osteoarthritis. The loading of an analgesic and non-steroidal anti-inflammatory drug into the same hydrogel could provide the long-term anti-inflammatory and analgesic treatment required to control the swelling and pain. This could make subcutaneous treatment with hydrogels a viable alternative to cortisone injections currently used by medical practitioners to treat arthritis without the spike in pain commonly caused following cortisone administration.

7. References

1. Jain, K., *Nanobiotechnology-based strategies for crossing the blood-brain barrier*. 2012; Vol. 7, p 1225-33.
2. Truven Health Analytics Inc How To Give A Subcutaneous Injection. <https://www.drugs.com/cg/how-to-give-a-subcutaneous-injection.html> (accessed November 1).
3. Truven Health Analytics Inc How To Give An Intramuscular Injection. <https://www.drugs.com/cg/how-to-give-an-intramuscular-injection.html> (accessed November 1).
4. Delmer, D. P.; Amor, Y., Cellulose biosynthesis. *The Plant Cell* **1995**, 7 (7), 987-1000.
5. Al Mualla, S., Farahat, R., Basmaji, P., de Olyveira, G.M., Costa, L.M.M., da Costa Oliveira, J.D and Francozo, G.B., Study of Nanoskin ECM-Bacterial Cellulose Wound Healing/United Arab Emirates. *Journal of Biomaterials and Nanobiotechnology* **2016**, 7, 109-117.
6. Riviere, J. E.; Papich, M. G., *Veterinary pharmacology and therapeutics*. 9th ed.; Wiley-Blackwell: Ames, Iowa, 2009; p xvi, 1524.
7. Naseri, N.; Deepa, B.; Mathew, A. P.; Oksman, K.; Girandon, L., Nanocellulose-Based Interpenetrating Polymer Network (IPN) Hydrogels for Cartilage Applications. *Biomacromolecules* **2016**, 17 (11), 3714-3723.
8. Tahiri, C.; Vignon, M. R., TEMPO-oxidation of cellulose: Synthesis and characterisation of polyglucuronans. *Cellulose* **2000**, 7 (2), 177-188.
9. Li, S.; Lee, P. S., Development and applications of transparent conductive nanocellulose paper. *Science and Technology of Advanced Materials* **2017**, 18 (1), 620-633.
10. HUA, K. Nanocellulose for Biomedical Applications. Uppsala, Uppsala University, 2016.
11. Jozala, A. F.; de Lencastre-Novaes, L. C.; Lopes, A. M.; de Carvalho Santos-Ebinuma, V.; Mazzola, P. G.; Pessoa-Jr, A.; Grotto, D.; Gerenutti, M.; Chaud, M. V., Bacterial nanocellulose production and application: a 10-year overview. *Applied Microbiology and Biotechnology* **2016**, 100 (5), 2063-2072.
12. Moritz, S.; Wiegand, C.; Wesarg, F.; Hessler, N.; Muller, F. A.; Kralisch, D.; Hipler, U. C.; Fischer, D., Active wound dressings based on bacterial nanocellulose as drug delivery system for octenidine. *Int J Pharmaceut* **2014**, 471 (1-2), 45-55.
13. George, J.; Sabapathi, S., Cellulose nanocrystals: synthesis, functional properties, and applications. *Nanotechnology, Science and Applications* **2015**, 8, 45-54.

14. Kalia, S.; Boufi, S.; Celli, A.; Kango, S., Nanofibrillated cellulose: surface modification and potential applications. *Colloid and Polymer Science* **2014**, 292 (1), 5-31.
15. Bordenave, N.; Grelier, S.; Coma, V., Advances on Selective C-6 Oxidation of Chitosan by TEMPO. *Biomacromolecules* **2008**, 9 (9), 2377-2382.
16. Khosravi-Darani, K.; Koller, M.; Akramzadeh, N.; Mortazavian, A. M., Bacterial nanocellulose: biosynthesis and medical application. *Biointerface Research in Applied Chemistry* **2016**, 6 (5), 1511-1516.
17. Foresti, M. L.; Cerrutti, P.; Vazquez, A., Bacterial Nanocellulose: Synthesis, Properties and Applications. In *Polymer Nanocomposites Based on Inorganic and Organic Nanomaterials*, John Wiley & Sons, Inc.: 2015; pp 39-61.
18. Thomson, F.; Naysmith, M.; Lindsay, A., Managing drug therapy in patients receiving enteral and parenteral nutrition. *Hosp Pharm* **2000**, 7 (6).
19. SherriOgston-Tuck, Subcutaneous injection technique: an evidence-based approach. *Nursing Standard* **2014**, 29 (3), 53-58.
20. BarbaraWorkman, Safe injection techniques. *Nursing Standard* **1999**, 13 (39), 47-53.
21. Jorfi, M.; Foster, E. J., Recent advances in nanocellulose for biomedical applications. *Journal of Applied Polymer Science* **2015**, 132 (14), n/a-n/a.
22. Hardy, J. G.; Lee, S. W.; Wilson, C. G., Intranasal drug delivery by spray and drops. *Journal of Pharmacy and Pharmacology* **1985**, 37 (5), 294-297.
23. Szekalska, M.; Puci; #x142; owska, A.; Szyma; #x144; ska, E.; Ciosek, P.; Winnicka, K., Alginate: Current Use and Future Perspectives in Pharmaceutical and Biomedical Applications. *International Journal of Polymer Science* **2016**, 2016, 17.
24. Tsigos, I.; Martinou, A.; Kafetzopoulos, D.; Bouriotis, V., Chitin deacetylases: new, versatile tools in biotechnology. *Trends in Biotechnology* **18** (7), 305-312.
25. Iqbal, A., *Production and characterization of Chitosan from shrimp waste*. 2015; Vol. 12.
26. Ilium, L., Chitosan and Its Use as a Pharmaceutical Excipient. *Pharmaceutical Research* **1998**, 15 (9), 1326-1331.
27. Cabral, J. D.; Moratti, S. C., Advances in Biomedical Hydrogels. *Chemistry in New Zealand* **2012**, 76 (2), 44-48.
28. Gulrez, S. K. H.; Al-Assaf, S., *Hydrogels: Methods of Preparation, Characterisation and Applications*. 2011.
29. Chirani, N.; Yahia, L. H.; Gritsch, L.; Motta, F. L.; Chirani, S.; Faré, S., History and Applications of Hydrogels. *Journal of Biomedical Sciences* **2015**, 4 (2), 1-23.

30. Maitra, J.; Shukla, V. K., Cross-linking in Hydrogels - A Review. *American Journal of Polymer Science* **2014**, *4* (2), 25-31.
31. Morozowich, N. L.; Nichol, J. L.; Allcock, H. R., Hydrogels based on schiff base formation between an amino-containing polyphosphazene and aldehyde functionalized-dextrans. *Journal of Polymer Science Part A: Polymer Chemistry* **2016**, *54* (18), 2984-2991.
32. Techawanitchai, P.; Idota, N.; Uto, K.; Ebara, M.; Aoyagi, T., A smart hydrogel-based time bomb triggers drug release mediated by pH-jump reaction. *Science and Technology of Advanced Materials* **2012**, *13* (6), 064202.
33. (a) Stein, C.; Schäfer, M.; Machelska, H., Attacking pain at its source: new perspectives on opioids. *Nature Medicine* **2003**, *9*, 1003; (b) Stein, C.; Lang, L. J., Peripheral mechanisms of opioid analgesia. *Current Opinion in Pharmacology* **2009**, *9* (1), 3-8.
34. Singh, P. M. Pharmacology of analgesic drugs in birds : thesis in fulfilment of the degree of Doctor of Philosophy in Animal Science. Ph. D., Massey University, 2011.
35. Zaveri, N., Peptide and nonpeptide ligands for the nociceptin/orphanin FQ receptor ORL1: Research tools and potential therapeutic agents. *Life sciences* **2003**, *73* (6), 663-678.
36. Pokorski, M. Respiratory regulation -- The molecular approach. <http://ezproxy.massey.ac.nz/login?url=http://dx.doi.org/10.1007/978-94-007-4549-0>.
37. Offermanns, S.; Rosenthal, W., *Encyclopedia of molecular pharmacology*. 2nd ed.; Springer: Berlin ; New York, 2008.
38. Orsini, J. A., *Butorphanol tartrate: pharmacology and clinical indications*. . 1988; Vol. 10.
39. Mansour, A.; Khachaturian, H.; Lewis, M. E.; Akil, H.; Watson, S. J., Anatomy of CNS opioid receptors. *Trends in Neurosciences* **1988**, *11* (7), 308-314.
40. Hawkins, M. G.; Paul-Murphy, J., Avian analgesia. *Vet Clin North Am Exot Anim Pract* **2011**, *14* (1), 61-80.
41. (a) Singh, P.; Johnson, C.; Gartrell, B.; Mitchinson, S.; Chambers, P., *Papers: Pharmacokinetics of butorphanol in broiler chickens*. 2011; Vol. 168, p 588; (b) Riggs, S. M.; Hawkins, M. G.; Craigmill, A. L.; Kass, P. H.; Stanley, S. D.; Taylor, I. T., Pharmacokinetics of butorphanol tartrate in red-tailed hawks (*Buteo jamaicensis*) and great horned owls (*Bubo virginianus*). *American Journal of Veterinary Research* **2008**, *69* (5), 596-603.
42. Clancy, M. M.; KuKanich, B.; Sykes Iv, J. M., Pharmacokinetics of butorphanol delivered with an osmotic pump during a seven-day period in common peafowl (*Pavo cristatus*). *American Journal of Veterinary Research* **2015**, *76* (12), 1070-1076.
43. Lanieste, D.; Guzman, D. S.-M.; Knych, H. K.; Smith, D. A.; Mosley, C.; Paul-Murphy, J. R.; Beaufrère, H., Pharmacokinetics of butorphanol tartrate in a long-acting

poloxamer 407 gel formulation administered to Hispaniolan Amazon parrots (*Amazona ventralis*). *American Journal of Veterinary Research* **2017**, 78 (6), 688-694.

44. Paul-Murphy, J. R.; Krugner-Higby, L. A.; Tourdot, R. L.; Sladky, K. K.; Klauer, J. M.; Keuler, N. S.; Brown, C. S.; Heath, T. D., Evaluation of liposome-encapsulated butorphanol tartrate for alleviation of experimentally induced arthritic pain in green-cheeked conures (*Pyrrhura molinae*). *American Journal of Veterinary Research* **2009**, 70 (10), 1211-1219.

45. Fenwick, N.; Griffin, G.; Gauthier, C., The welfare of animals used in science: How the “Three Rs” ethic guides improvements. *The Canadian Veterinary Journal* **2009**, 50 (5), 523-530.

46. Clovis, C. About New Therapeutic Uses. National Center for Advancing Translational Sciences. <https://ncats.nih.gov/ntu/about> (accessed 5-9-2017).

47. Brem, H.; Tomic-Canic, M., Cellular and molecular basis of wound healing in diabetes. *The Journal of Clinical Investigation* **2007**, 117 (5), 1219-1222.

48. Lin, N.; Dufresne, A., Nanocellulose in biomedicine: Current status and future prospect. *European Polymer Journal* **2014**, 59, 302-325.

49. Ishikawa, T.; Koizumi, N.; Mukai, B.; Utoguchi, N.; Fujii, M.; Matsumoto, M.; Endo, H.; Shirotake, S.; Watanabe, Y., Pharmacokinetics of Acetaminophen from Rapidly Disintegrating Compressed Tablet Prepared Using Microcrystalline Cellulose (PH-M-06) and Spherical Sugar Granules. *Chemical and Pharmaceutical Bulletin* **2001**, 49 (2), 230-232.

50. Hyon, S.-H.; Cha, W.-I.; Ikada, Y.; Kita, M.; Ogura, Y.; Honda, Y., Poly(vinyl alcohol) hydrogels as soft contact lens material. *Journal of Biomaterials Science, Polymer Edition* **1994**, 5 (5), 397-406.

51. Konczewicz, W.; Zimniewska, M.; Valera, M. A., The selection of a retting method for the extraction of bast fibers as response to challenges in composite reinforcement. *Textile Research Journal* 0 (0), 0040517517716902.

52. Coskun, O., Separation techniques: Chromatography. *Northern Clinics of Istanbul* **2016**, 3 (2), 156-160.

53. Dixon, P. F.; Stoll, M. S.; Lim, C. K., High Pressure Liquid Chromatography in Clinical Chemistry: A Review. *Annals of Clinical Biochemistry* **1976**, 13 (1-6), 409-432.

54. Saito, T.; Kimura, S.; Nishiyama, Y.; Isogai, A., Cellulose Nanofibers Prepared by TEMPO-Mediated Oxidation of Native Cellulose. *Biomacromolecules* **2007**, 8 (8), 2485-2491.

55. Lin, N.; Bruzzese, C.; Dufresne, A., TEMPO-Oxidized Nanocellulose Participating as Crosslinking Aid for Alginate-Based Sponges. *Acs Appl Mater Inter* **2012**, 4 (9), 4948-4959.

56. Zhang, Y.; Huo, M.; Zhou, J.; Xie, S., PKSolver: An add-in program for pharmacokinetic and pharmacodynamic data analysis in Microsoft Excel. *Computer Methods and Programs in Biomedicine* **2010**, *99* (3), 306-314.
57. Barriga, S., 2,2,6,6-Tetramethylpiperidin-1-oxyl (TEMPO). *Synlett* **2001**, *2001* (04), 0563.
58. Wiederschain, G. Y., Principles and practice of bioanalysis (2nd Edn.). *Biochemistry (00062979)* **2008**, *73* (12), 1351-1351.
59. Klein, M.; Preud'homme, H.; Bueno, M.; Pannier, F., Study of volatile selenium metabolites stability in normal urine: effects of sample handling and storage conditions. *Journal of Analytical Atomic Spectrometry* **2011**, *26* (3), 602-607.

8. Appendices

Appendix i. Timesheets for chicken sampling (Gel).

Chicken	Day	G1	Hours since start	G2	Hours since start	G3	Hours since start
Start Time	Wed	27/09/2017 10:10	0	27/09/2017 10:12	0	27/09/2017 10:14	0
15min	Wed	27/09/2017 10:27	0.283333333	27/09/2017 10:30	0.3	27/09/2017 10:33	0.316666667
30min	Wed	27/09/2017 10:40	0.5	27/09/2017 10:43	0.516666667	27/09/2017 10:45	0.516666667
1hr	Wed	27/09/2017 11:11	1.016666667	27/09/2017 11:13	1.016666667	27/09/2017 11:15	1.016666667
2hr	Wed	27/09/2017 12:10	2	27/09/2017 12:12	2	27/09/2017 12:15	2.016666667
4hr	Wed	27/09/2017 14:18	4.133333333	27/09/2017 14:20	4.133333333	27/09/2017 14:23	4.15
8hr	Wed	27/09/2017 18:12	8.033333333	27/09/2017 18:24	8.2	27/09/2017 18:32	8.3
16hr	Thu	28/09/2017 2:05	15.916666667	28/09/2017 2:08	15.933333333	28/09/2017 2:14	16
24hr	Thu	28/09/2017 8:42	22.533333333	28/09/2017 8:45	22.55	28/09/2017 8:51	22.616666667
36hr	Fri	29/09/2017 0:27	38.283333333	29/09/2017 0:30	38.3	29/09/2017 0:33	38.316666667
48hr	Fri	29/09/2017 9:35	47.416666667	29/09/2017 9:37	47.416666667	29/09/2017 9:41	47.45
72hr	Sat	30/09/2017 9:42	71.533333333	30/09/2017 9:49	71.616666667	30/09/2017 9:54	71.666666667
96hr	Sun	1/10/2017 9:34	95.4	1/10/2017 9:39	95.45	1/10/2017 9:43	95.483333333

Chicken	Day	G4	Hours since start	G5	Hours since start	G6	Hours since start
Start Time	Thu	28/09/2017 9:39	0	28/09/2017 9:41	0	28/09/2017 9:42	0
15min	Thu	28/09/2017 9:52	0.216666667	28/09/2017 9:58	0.283333333	28/09/2017 10:00	0.3
30min	Thu	28/09/2017 10:09	0.5	28/09/2017 10:12	0.516666667	28/09/2017 10:13	0.516666667
1hr	Thu	28/09/2017 10:38	0.983333333	28/09/2017 10:41	1	28/09/2017 10:52	1.166666667
2hr	Thu	28/09/2017 11:46	2.116666667	28/09/2017 11:49	2.133333333	28/09/2017 11:52	2.166666667
4hr	Thu	28/09/2017 13:41	4.033333333	28/09/2017 13:45	4.066666667	28/09/2017 13:50	4.133333333
8hr	Thu	28/09/2017 17:38	7.983333333	28/09/2017 17:43	8.033333333	28/09/2017 17:48	8.1
16hr	Fri	29/09/2017 1:04	15.416666667	29/09/2017 1:10	15.483333333	29/09/2017 1:16	15.566666667
24hr	Fri	29/09/2017 8:45	23.1	29/09/2017 9:27	23.766666667	29/09/2017 9:31	23.816666667
36hr	Sat	30/09/2017 0:14	38.583333333	30/09/2017 0:23	38.7	30/09/2017 0:26	38.733333333
48hr	Sat	30/09/2017 9:49	48.166666667	30/09/2017 10:02	48.35	30/09/2017 10:05	48.383333333
72hr	Sun	1/10/2017 9:49	72.166666667	1/10/2017 9:55	72.233333333	1/10/2017 10:00	72.3
96hr	Mon	2/10/2017 9:43	96.066666667	2/10/2017 9:56	96.25	2/10/2017 9:58	96.266666667

Appendix ii. Timesheets for chicken sampling (No Gel).

Chicken	Day	NG1	Hours since start	NG2	Hours since start
Start Time	Fri	29/09/2017 9:55	0	29/09/2017 9:56	0
15min	Fri	29/09/2017 10:10	0.25	29/09/2017 10:11	0.25
30min	Fri	29/09/2017 10:26	0.516666667	29/09/2017 10:28	0.533333333
1hr	Fri	29/09/2017 10:55	1	29/09/2017 10:57	1.016666667
2hr	Fri	29/09/2017 11:53	1.966666667	29/09/2017 11:56	2
4hr	Fri	29/09/2017 14:03	4.133333333	29/09/2017 14:05	4.15
8hr	Fri	29/09/2017 17:57	8.033333333	29/09/2017 18:00	8.066666667
16hr	Sat	30/09/2017 0:50	14.916666667	30/09/2017 0:53	14.95
24hr	Sat	30/09/2017 10:13	24.3	30/09/2017 10:15	24.316666667
36hr	Sat	30/09/2017 21:46	35.85	30/09/2017 21:48	35.866666667
48hr	Sun	1/10/2017	48.25	1/10/2017	48.283333333

Chicken	Day	NG3	Hours since start	NG4	Hours since start	NG5	Hours since start	NG6	Hours since start
Start Time	Mon	2/10/2017	0	2/10/2017	0	2/10/2017	0	2/10/2017	0
15min	Mon	2/10/2017	0.25	2/10/2017	0.25	2/10/2017	0.266666667	2/10/2017	0.266666667
30min	Mon	2/10/2017	0.6	2/10/2017	0.65	2/10/2017	0.666666667	2/10/2017	0.7
1hr	Mon	2/10/2017	1.033333333	2/10/2017	0.966666667	2/10/2017	1.033333333	2/10/2017	1.05
2hr	Mon	2/10/2017	2.016666667	2/10/2017	2.033333333	2/10/2017	2.05	2/10/2017	2.05
4hr	Mon	2/10/2017	4.033333333	2/10/2017	4.033333333	2/10/2017	4.033333333	2/10/2017	4.05
8hr	Mon	2/10/2017	7.933333333	2/10/2017	7.95	2/10/2017	7.966666667	2/10/2017	8
16hr	Tue	3/10/2017	15.516666667	3/10/2017	15.566666667	3/10/2017	15.583333333	3/10/2017	15.6
24hr	Tue	3/10/2017	23.75	3/10/2017	24.116666667	3/10/2017	24.366666667	3/10/2017	24.216666667
36hr	Wed	4/10/2017	38.35	4/10/2017	38.383333333	4/10/2017	38.4	4/10/2017	38.433333333
48hr	Wed	4/10/2017	47.983333333	4/10/2017	47.983333333	4/10/2017	48	4/10/2017	48